EXPERIMENTAL MODELLING OF RESISTANCE SPOT WELDING OF ADVANCED HIGH STRENGTH STEELS

GELİŞMİŞ YÜKSEK DAYANIMLI ÇELİKLERDE PUNTA KAYNAĞININ DENEYSEL MODELLENMESİ

ALİ BERKCAN KUTLUTÜRK

ASST. PROF. MEHMET OKAN GÖRTAN

Supervisor

Submitted to

Graduate School of Science and Engineering of Hacettepe University

as a Fulfillment to the Requirements

for the Award of the Degree of Master of Science

in Mechanical Engineering

2023

ABSTRACT

EXPERIMENTAL MODELLING OF RESISTANCE SPOT WELDING OF ADVANCED HIGH STRENGTH STEELS

Ali Berkcan KUTLUTÜRK

Master of Science, Department of Mechanical Engineering

Supervisor: Asst. Prof. Mehmet Okan GÖRTAN

January 2023, 50 pages

The use of advanced high strength steels (AHSS) is becoming more dominant in the automotive industry due to the excellent balance of strength and lightness of these steels. Although the use of AHSS metals is increasing, there are not enough studies in the scientific literature on resistance spot welding, which is the basic joining method used in automobile production, of AHSS metals each other or to other metals. In this study, MS1500, an AHSS metal, dual-phase steel (DP800) and unalloyed mild steel (DD11) are used. The welding joints created with using single and double pulse resistance spot welding with variable electric currents, which are the results of joining the MS1500-DD11 and MS1500-DP800 metal pairs, respectively, have been investigated from many different aspects by experimental modeling. In resistance spot welding applications where AHSS metals are used, due to the high alloying contents of these metals, it has been observed that interfacial failure occurs, which is absolutely undesirable in the automotive industry, as a failure mode up to the critical current value that will cause expulsion as a result of single pulse. While the first pulse increases the contact area between metals, the second pulse ensures that the weld nugget area of the joint, which is formed after the first

pulse, is re-melted. By this way, it is observed that, metals in the nugget zone becomes annealed and nugget size increases, it enables to change the failure modes to the desired mode, pullout failure. When the experimental results such as tensile-shear strength, failure energy, and failure mode analysis obtained after the tensile-shear tests are examined, both the strength of the joints increased and the deviations in the results decreased with the second current, which was gradually increased, following a first current applied just below the expulsion limit in the first pulse. This trend continues until appearance of expulsion because of the second pulse electric current. The optimum welding parameters are determined by evaluating the strength values corresponding to different welding parameters obtained as a result of the experiments, the change of failure modes, the geometric measurements of the weld nugget area and the hardness measurements along the nugget.

Keywords: Resistance spot welding, double pulse, nugget formation, advanced high strength steel, dual-phase steel, unalloyed mild steel, failure modes.

ÖZET

GELİŞMİŞ YÜKSEK DAYANIMLI ÇELİKLERDE PUNTA KAYNAĞININ DENEYSEL MODELLENMESİ

Ali Berkcan KUTLUTÜRK

Yüksek Lisans, Makine Mühendisliği Bölümü

Tez Danışmanı: Dr. Öğr. Üyesi Mehmet Okan GÖRTAN

Ocak 2023, 50 sayfa

Gelişmiş yüksek dayanımlı çeliklerin kullanımı, bu çeliklerin mükemmel bir dayanım ve hafiflik dengeleri nedeniyle otomotiv endüstrisinde giderek daha baskın hale gelmektedir. Gelişmiş yüksek dayanımlı çeliklerin kullanımları giderek artmakta olmasına rağmen, bilimsel literatürde otomobil üretiminde kullanılan temel montaj metodu olan direnç punta kaynağı ile birbirlerine ya da başka metallere montajlanması ile ilgili yeterli çalışma bulunmamaktadır. Bu çalışmada, bir gelişmiş yüksek dayanımlı çelik olan MS1500, çift fazlı çelik (DP800) ve alaşımsız yumuşak çelik (DD11) kullanılmıştır. Sırasıyla MS1500-DD11 ve MS1500-DP800 metal çiftlerinin, değişken elektrik akımları ile tek ve çift adımlı direnç punta kaynağı kullanarak montajlanması sonucunda ortaya çıkan bağlantılar deneysel modelleme ile, birçok açıdan incelenmiştir. Gelişmiş yüksek dayanımlı çeliklerin kullanıldığı direnç punta kaynağı uygulamalarında, bu metallerin yüksek alaşım içerikleri sebebiyle, tek adım sonucu fışkırmaya neden olacak akım değerine kadar kırılma modu olarak otomotiv sanayisinde istenmeyen arayüz kırılması oluştuğu gözlemlenmiştir. İlk adım metaller arası temas alanını arttırırken, ikinci adım ile birlikte, ilk adım sonrası ortaya çıkan bağlantının kaynak dolgusu bölgesinde tekrardan bir ergime gerçekleşerek alanın tavlanması sonucunda kırılma modlarının istenen mod

olan düğmelenmeye çevrilmesi sağlanır. Çekme-makaslama testi sonrası elde edilen çekme-makaslama dayanımı, kırılma enerjisi, kırılma modu analizi gibi deney sonuçları incelendiğinde, ilk adımda fışkırma limitinin hemen altında uygulanan bir ilk adım akımını takiben, giderek arttırılan ikinci adım akımı ile bağlayıcının hem dayanımı artmış hem de sonuçlardaki sapma giderek azalmıştır. Bu trend ikincil akımda fışkırma yaşanan değere gelinene kadar devam etmiştir. Deneylerin sonucunda elde edilen değişik kaynak parametrelerine karşılık gelen dayanım değerleri, kırım modlarının değişimi, kaynak dolgusu bölgesinin geometrik ölçümleri ve kaynak dolgusu boyunca sertlik ölçümleri değerlendirilerek optimum kaynak parametresi tespiti yapılmıştır.

Anahtar Kelimeler: Direnç punta kaynağı, iki adım, kaynak dolgusu oluşumu, gelişmiş yüksek dayanımlı çelik, çift fazlı çelik, alaşımsız yumuşak çelik, kırılma modu.

ACKNOWLEDGEMENTS

I would like to express my sincere gratitude to my supervisor Asst. Prof. Mehmet Okan GÖRTAN for his advice, guidance, and recommendations throughout this study.

I would like to thank my friends for encouraging me all the time.

Special thanks to my lovely wife Dünya Berrak KUTLUTÜRK for her kindness, patience and supports during all these difficult times in my life.

Finally, I would like to express my deepest love to my family for their endless support and understanding.

TABLE OF CONTENTS

LIST OF FIGURES

LIST OF TABLES

SYMBOLS AND ABBREVIATIONS

Symbols

I	Electric Current
R	Electrical Resistance
g	Gram
Q	Heat
Hz	Hertz
kVA	Kilo Volt-Amperes
kA	Kiloampere
kg	Kilogram
kN	Kilonewton
MPa	Megapascal
μ	Micron
mm	Millimeter
ms	Millisecond
s	Second
t_{sheet}	Sheet Thickness
t	Time
w_d	Weld Nugget Size

Abbreviations

AHSS	Advanced High Strength Steel
AC	Alternative Current
CNC	Computer Numerical Control
DP800	Dual-Phase Steel

HAZ	Heat Affected Zone
IF	Interfacial Failure
ISO	International Organization for Standardization
MS1500	Martensitic Steel
DD11	Mild Unalloyed Steel
PF	Pullout Failure
RSW	Resistance Spot Welding
SIC	Silicon Carbide
TSS	Tensile-Shear Strength

1. INTRODUCTION

In today's world, as in almost every sector, competition in the automotive sector is increasing like never before. For this reason, it is very important to increase the worldwide market share to survive in the sector for a long time. In addition, it is an inevitable necessity to both reduce costs and increase production speeds to increase profitability. The main structural materials used in the automobile industry are steel sheet metals. The chassis, which is formed by assembling these metals to each other, constitutes the main structure of the automobiles. In addition to many other joining technologies, the most widely used joining method in automobile production is resistance spot welding.

Resistance spot welding (RSW) is the basic joining method of automotive production that allows two or more sheet metals to be permanently joined to each other by converting electrical current into heat energy. Thousands of resistance spot welding are used in an automobile. In addition, resistance spot welding is an extremely fast, easily automated and robotized and cheap joining method. Furthermore, a considerable amount of robust results can be obtained compared to other welding types. This consistency and robustness arise because it requires less operator skill level.

In order to make more environmentally friendly and economical cars, lighter structures should be used. In this way, a more livable future can be created by reducing carbon gas emissions. However, while doing this, it is obligatory to meet very strict safety criteria. As a solution to this problem, the use of light and strong materials, called advanced high strength steels (AHSS), with excellent crashworthiness properties, is gradually increasing. Making lightweight designs without sacrificing strength with the use of AHSS is the new trend in automobile design.

Although there are many experimental and numerical studies on resistance spot welding in the literature, studies using advanced high strength steels are relatively new and few in number. With the widespread use of AHSS materials and their dominance in the sector, it is a necessity that the quantity and quality of these studies increase. In this study,

resistance spot welding of advanced high strength steels has been experimentally modeled and investigated in detail and the weld formed as a result of joining both mild steel and dual phase steels with resistance spot welding and AHSS are examined. It is aimed to determine the optimum welding parameters in terms of welding current to be used to obtain the desired welding joint properties, strength and failure mode by using both single pulse resistance spot welding and double pulse spot welding methods.

This study starts with the introduction part and continues with the state of the art section, which explains the basic principles of the resistance spot welding process, the materials used, the factors affecting the resistance spot welding and the failure modes of joints created using the studies in the scientific literature. The following is the motivation and methodology section, which includes the motivation behind the study, the details of the materials used, the methods, and all the details of the experimental process from specimen production to preparation for examination. The results of the tensile-shear strength tests, the reasons for the failures, the experimental outputs such as the detailed geometric measurements of the resistance spot welding regions and the hardness distribution values are given in the experimental results section. The evaluations that emerged as a result of the whole study, the outputs, future studies and contributions are summarized in the conclusions and outlook section.

2. STATE OF THE ART

2.1. Advanced High Strength Steels

Many different types of steel are used in the automotive industry, which can be classified by separating them from each other by their strength and microstructure. The tensile strength values of the steels defined as advanced high strength steel are at least 440 MPa. In addition, AHSS steels, unlike other steels, contain at least one or more phases in addition to ferrite, pearlite, cementite phases in their microstructure. They may contain martensite, bainite, austenite or retained austenite in their microstructure to achieve the specific mechanical properties needed. As seen in the Figure 2-1, The tensile strength values of advanced high strength steels can reach up to 2000 MPa. [1]

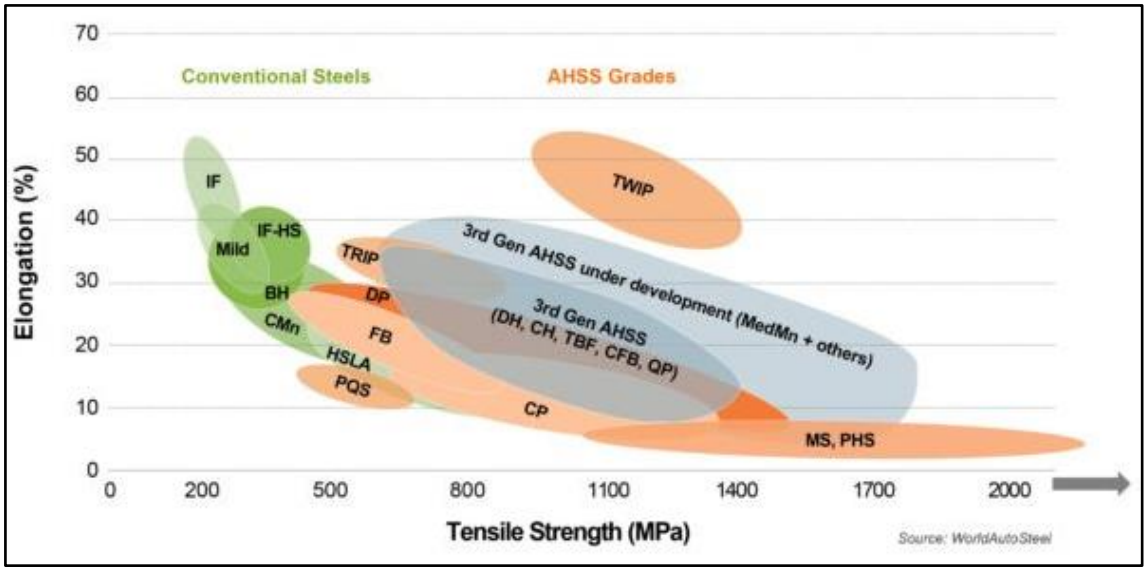

Figure 2-1: The Global Formability Diagram comparing strength and elongation of current and emerging steel grades. [1]

Advanced high strength steels (AHSS) are an economical solution used in the automotive industry that meets the safety and lightness criteria that are getting harder to meet day by day. AHSS not only has superior crashworthiness properties, but also stands out with its very good formability [2].

In today's world, besides the safety needs in automobile designs, the importance of fuel economy and reducing carbon gas emissions for a sustainable future is increasing. According to Cheah, reducing the weight of a vehicle by 10% will increase fuel economy by 4.9% [3]. However, reducing the vehicle weight by 100 kg will increase the safety risk by 3-4.5 percent in accidents. [4,5] Therefore, the use of AHSS metals instead of conventional steels has become quite common in the automotive industry. In this way, it has become possible to design and manufacture lighter, economical and environmentally friendly vehicles without sacrificing safety. Resistance spot welding is still the best solution for joining AHSS sheet metals together.

2.2. Resistance Spot Welding

During the manufacture of an automobile, thousands of resistance spot welding applications are made. In the event of an accident, the protection of the structural integrity of the car is directly related to the performance of these spot welds. Naturally, passenger safety is also related to the quality of these resistance spot welds [6].

Resistance Spot Welding (RSW) is a complex process based on the permanent joining of two or more conductive metals to each other by converting electrical current into heat energy, which is widely used especially in the automotive industry. Resistance spot welding is a very fast, easily automated, repeatable and robust production process compared to other welding types [7]. Usually, during resistance spot welding lower operator skill level is needed than for arc welding. According to Raoelison et al. (2014) [8], the formation of resistance spot welding depends on many parameters, the most important of which are the physical properties of the material used, the electrode force, the process time, the shape and the contact conditions of electrodes. Changes occur in the mechanical and metallurgical structure of the material during resistance spot welding. Therefore, resistance spot welding is a process that is strongly depended to the electrical, thermal, mechanical and metallurgical properties of the material. Schematic view of resistance spot welding process can be seen in Figure 2-2.

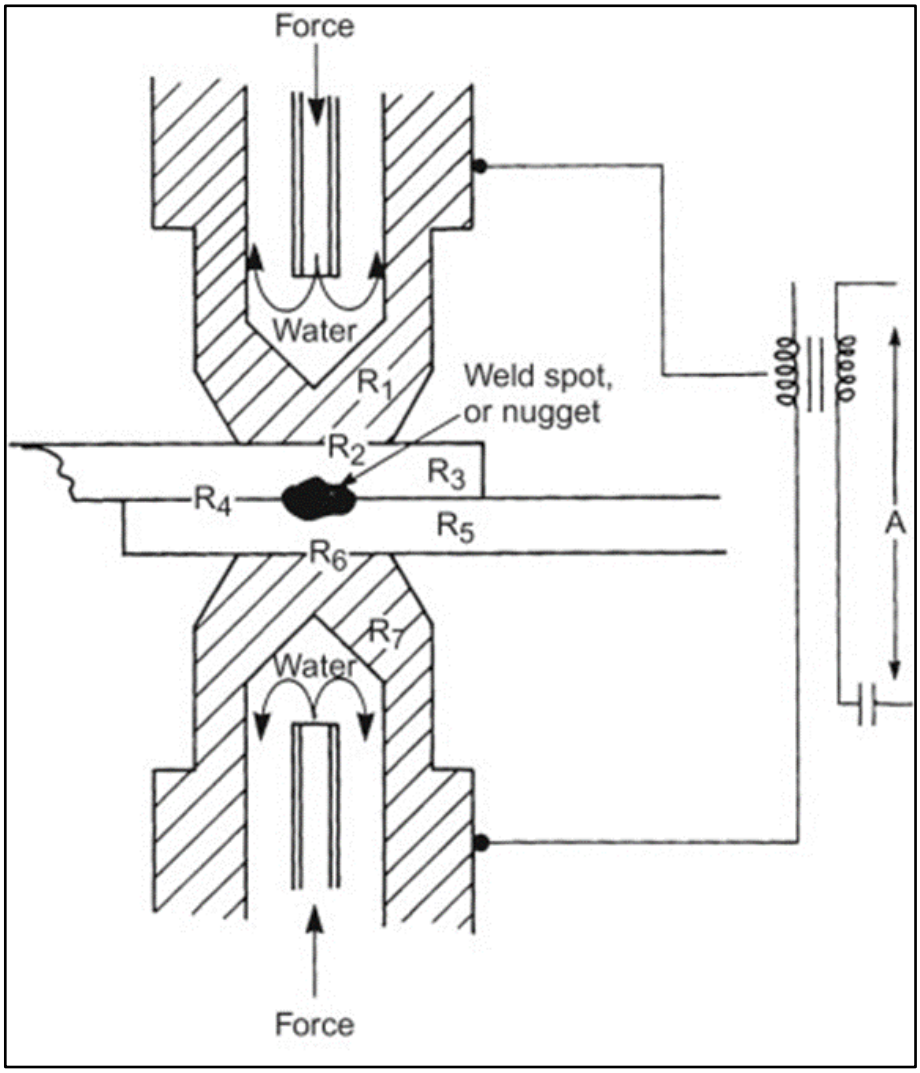

Figure 2-2: Schematic view of Resistance Spot Welding Process [9]

The quality and strength of the welding process is directly related to the size and metallurgical properties of the region formed at the center of the weld called the “nugget”. Eisazadeh et al. (2009) [7] states that quality and strength of resistance spot welding can be defined by the size and the shape of weld nuggets. Nugget size is the most dominant factor and there is a direct relationship between the heat generated during joint formation and the nugget size. Among the main factors determining the properties of the nugget region are the amount of current, the duration of the process, which is generally defined by the number of cycles, the material and thickness of the metals to be joined, the materials and the geometries of the electrodes, and the electrode force. In addition, the transmission (conduction, diffusion) and distribution of heat from the electrodes to the materials must be carefully studied to examine nugget formation.

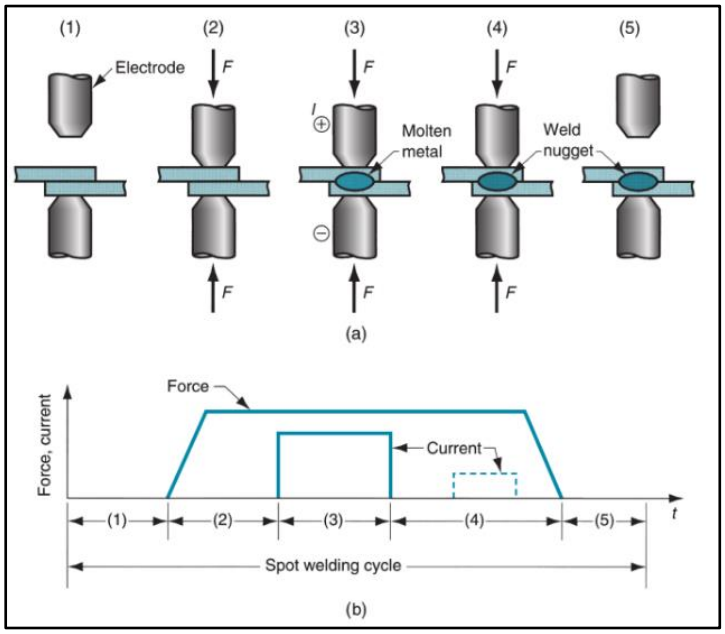

Figure 2-3: Fundamental steps of Resistance Spot Welding Process [10]

Resistance spot welding process mostly consists of combining 5 main steps as seen in Figure 2-3. The first step is the step of placing the parts to be spot welded, this step covers a very large part of the total process. Especially in the automotive industry, this step is carried out by robot arms and conveyor belts. In the second step, force is applied on the parts to be welded by means of electrodes. Generally, while one of the electrodes is fixed, the desired force is produced by the movement of the other. The third stage is the step where resistance spot welding is actually performed. In this step, low voltage and high current electricity is applied through electrodes, one of which is positive pole and one is negative pole. The process usually takes 10 cycles (200 ms except US). Meanwhile, while contact resistance decreases, material resistance gradually increases. Meanwhile, the total resistance reaches its highest value during operation.

$$Q = I^2 \, x \, R \, x \, t \qquad Eq.(1)$$

$$dQ = I\,(t)^2 \, x \, R(t) \, x \, dt \qquad Eq.(2)$$

A large amount of heat is generated across the sheet-to-sheet interface because initially a significant localized resistance is present at weld interface. The resulting heat initiates melting along this faying surface [11]. Resistance spot welding is based on Joule's first law that gives an expression for the amount of heat generated by a current flowing through a conductor. Generated heat can be expressed by the Eq. (1) where Q = heat generated, J (joule); I = current, A (ampere); R = electrical resistance, Ω (ohm) and t = time, s (second). The heat produced is directly proportional to the square of the current, the total resistance and time. In resistance spot welding very low voltage with high current is used because square term in Eq. (1) amplifies the effect of current [6]. Unfortunately, Eq. (1) is not enough to calculate the total heat generation because the multipliers in Eq. (1) are not constant during resistance spot welding. The amount of current flowing through system changes depending on the time. In addition, the total resistance also varies depending on the time. Therefore, as seen in Eq. (2), the equation must be integrated over time to find the total heat generation during the process.

During the process, very high temperatures are reached. In order to prevent the electrodes from melting or eroding, the electrodes are cooled with high flow liquid flow. In the fourth stage, the electric current is cut off and the molten material is solidified. As a result of solidification, nugget formation is completed. At the last stage, the force applied on the electrodes is removed and the resistance spot welding process is completed.

2.3. Geometric Properties of Resistance Spot Weld Nugget

Among the geometric properties of the nugget region, the parameter that has the most impact on the strength of the joint is the nugget size. So, it can be said that the ultimate goal of resistance spot welding is the formation of the nugget region because the properties of the nugget region determine the strength and toughness of the weld. Basic nugget parameters are visualized in Figure 2-4. Nugget size can be defined as the largest diameter of the diffusion (melting) zone. Nugget penetration is basically height of penetration of nugget. It is desired that nugget penetration should be as high as possible. However, it is not desired that nugget to reach to surface of material because this situation cause reduce in electrode life. Gap between sheets, indentation size and indentation height

are parameters that depend on electrode force and geometry. Other parameters are diffusion joint area size and heat affected zone size.

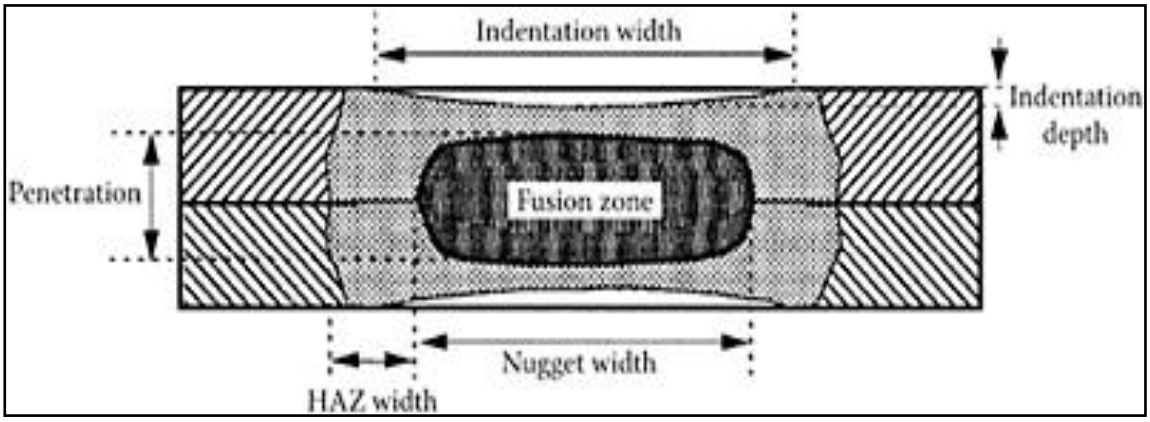

Figure 2-4: Nugget Parameters [12]

The geometric and metallurgical properties of the nugget, which largely determine the strength of the joint formed as a result of the resistance spot welding process, cannot be determined by visual inspection mostly. In resistance spot welding test methods, the joint is generally become unusable by appropriate methods and loses its load carrying capacity.

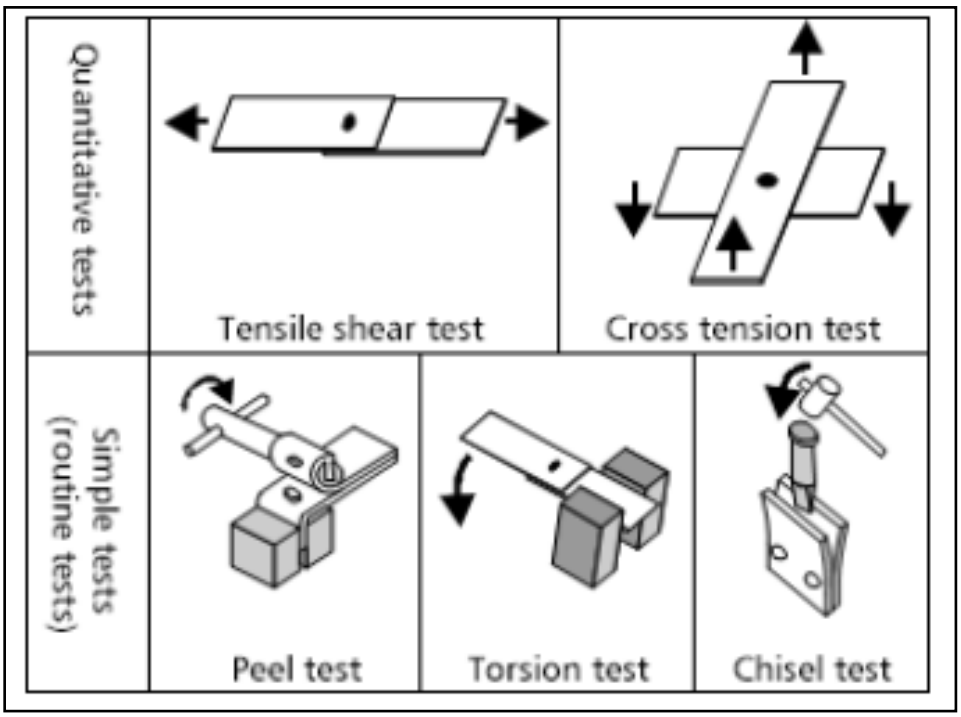

Figure 2-5: Testing methods of resistance spot welding [13]

Some testing methods of resistance spot welding joints can be seen in Figure 2-5. The sample obtained in this way is analyzed in the laboratory environment and the geometric and metallurgical properties of the nugget are determined.

2.4. Failure Modes of Resistance Spot Welds

In resistance spot welds, there are generally two types of failure modes: interfacial failure (IF) and pullout failure (PF). These failure modes can be seen in Figure 2-6 and Figure 2-7. Interfacial failure and partial interfacial failure are the types of failure to be avoided in the resistance spot welds.

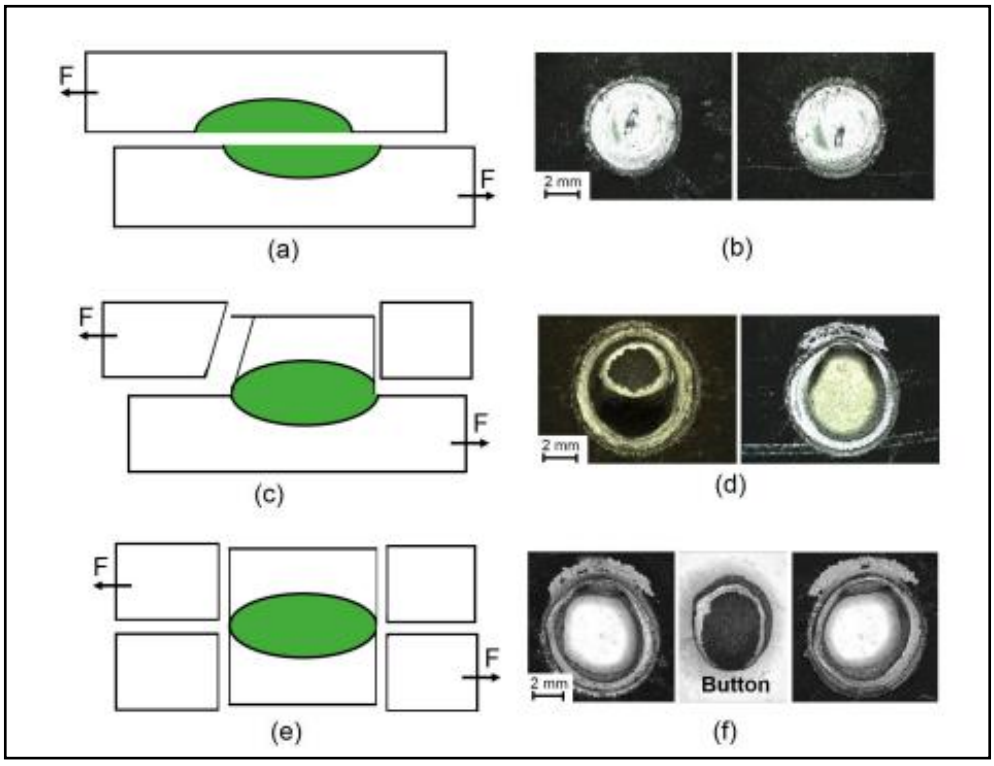

Figure 2-6: Failure modes of resistance spot weldings (a) schematic of interfacial fracture (IF); (b) failed IF joint; (c) schematic of pull-out fracture initiated at the transition zone between the fusion zone and upper-critical heat affected zone (d) failed corresponding PF joint (e) schematic of pull-out fracture initiated at the base metal (f) failed corresponding PF joint [14]

During interfacial failure, a crack starts in the weld nugget area of the joint and the load carrying capacity of the joint is decreased very quickly. This is definitely undesirable and should be avoided. During the pullout failure mode, the resistance spot weld starts to separate from the metals it connects. The energy dissipation is better due to the plastic deformation that occurs and the amount of force required to take the joint out of use is greater. [6]

The quality and performance of resistance spot welds are mainly related to the size of the weld nugget, the microstructure of the weld nugget and the heat affected zone. The larger the weld nugget size, the more robust the resistance spot weld will be.

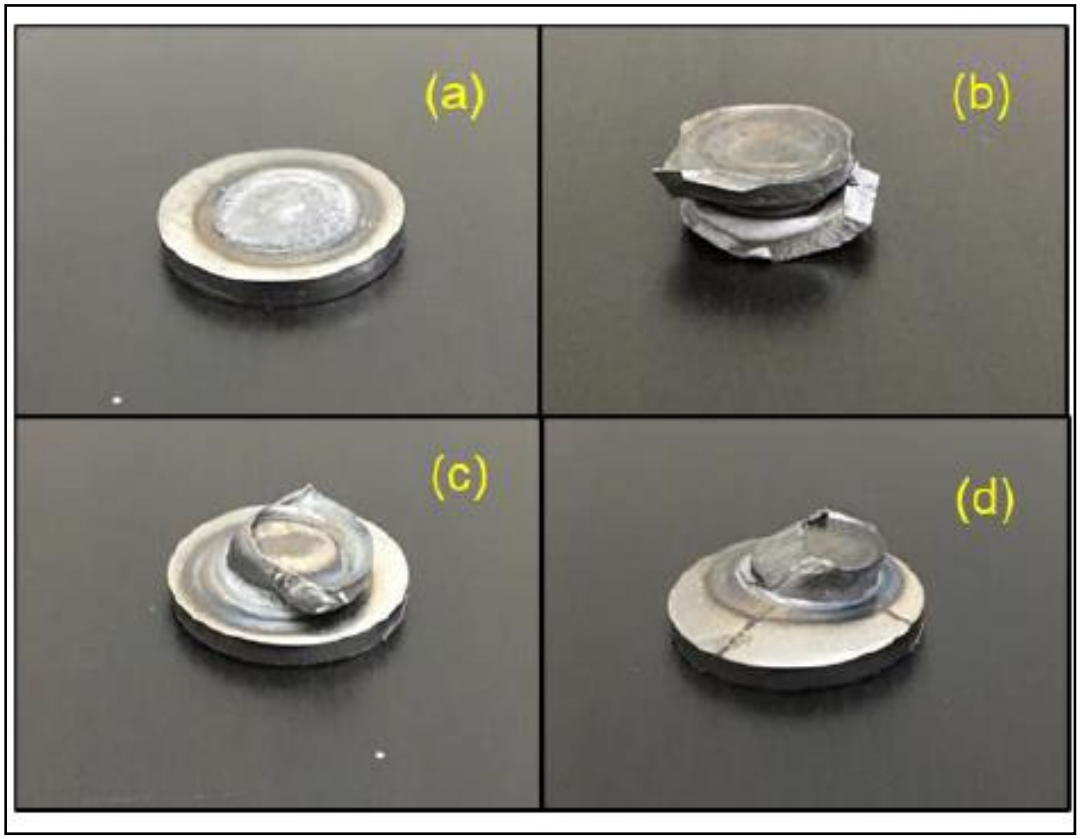

Figure 2-7: (a) Interfacial failure (b) pullout failure (c) partial interfacial failure (d) partial thickness-partial pullout failure [6]

One way to increase the weld nugget size is to increase the heat input. To increase the heat input, what needs to be done is to increase the welding current because the heat input is directly proportional to the square of the welding current as shown in Eq. (2). In the past, it was accepted in the industry that the weld nugget size should be at least four times the square root of the sheet metal thickness, as seen in Eq. (3), in order to stay away from the interracial failure mode (t_{sheet} is in mm). [15]

$$w_d \geq 4\sqrt{t_{sheet}} \qquad Eq.(3)$$

Because AHSS metals contain a high amount of alloying elements, they are very prone to contain a martensitic microstructure after processes such as resistance spot welding that require high heating and extremely rapid cooling. After resistance spot welding, a dense martensitic microstructure is observed in the weld center. Due to the low fracture toughness value of this martensitic structure in the weld area, it can be said that AHSS metals are more prone to experience interfacial failure mode after spot welding. Today, it is recommended to calculate the weld nugget size with the Eq. (4) instead of Eq. (3), both for this reason and due to the strict safety regulations today. [16]

$$w_d \geq 5\sqrt{t_{sheet}} \qquad Eq.(4)$$

Generally, there is a critical spot weld nugget dimension in the resistance spot welding process that switches failure mode from interfacial mode to pullout mode. However, AHSS metals are prone to fracture in pullout mode even at higher weld nugget dimensions. [17] The reason for this is that the microstructure is mostly heterogeneous martensitic and at the same time, higher welding currents cannot be achieved. Due to the high alloying elements in AHSS metals, their properties such as electrical resistance are different from other metals. For such reasons, AHSS metals tend to experience expulsion. This significantly reduces the maximum tensile yield load and energy dissipation capacity of the resistance spot weld. [18] As an example, acceptable welding current range of 15B22 hot stamped boron steel with 1.2 mm thick can be shown in the Figure 2-8. Lower acceptable limit of the nugget diameter is approximately 4.4 mm which calculated with

Eq. (3) and corresponding weld current can be shown. Higher acceptable limit can be seen where expulsion occurs.

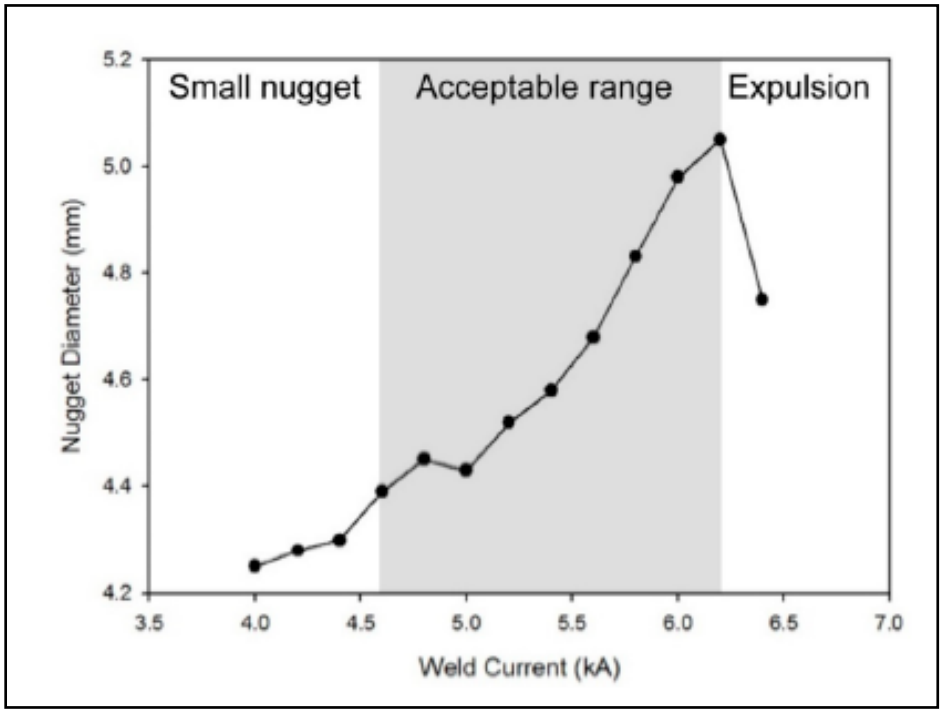

Figure 2-8: Welding current range of 15B22 [18]

2.5. Double Pulse Resistance Spot Welding

Double pulse resistance spot welding is used to increase the nugget size without causing expulsion. In this way, in addition to increasing the nugget size, it is also possible to change the microstructure of the weld nugget. As a result of the change in the microstructure of the weld nugget, the properties of the material such as ductility are improved, and the failure mode can also change.

With the first current pulse of resistance spot welding, the areas of the metals under the influence of heat melt completely. Afterwards, the metals cool very quickly and take on a brittle structure. This can be a factor that reduces the performance of the welding joint. Then, thanks to the second current pulse applied to prevent this, the microstructure in the nugget takes on a much more homogeneous structure. At the same time, nugget size increases because more material is exposed to the heating. In the Figure 2-9, cross-

sections of a single pulse and double pulse resistance spot welding joints can be seen. [19]

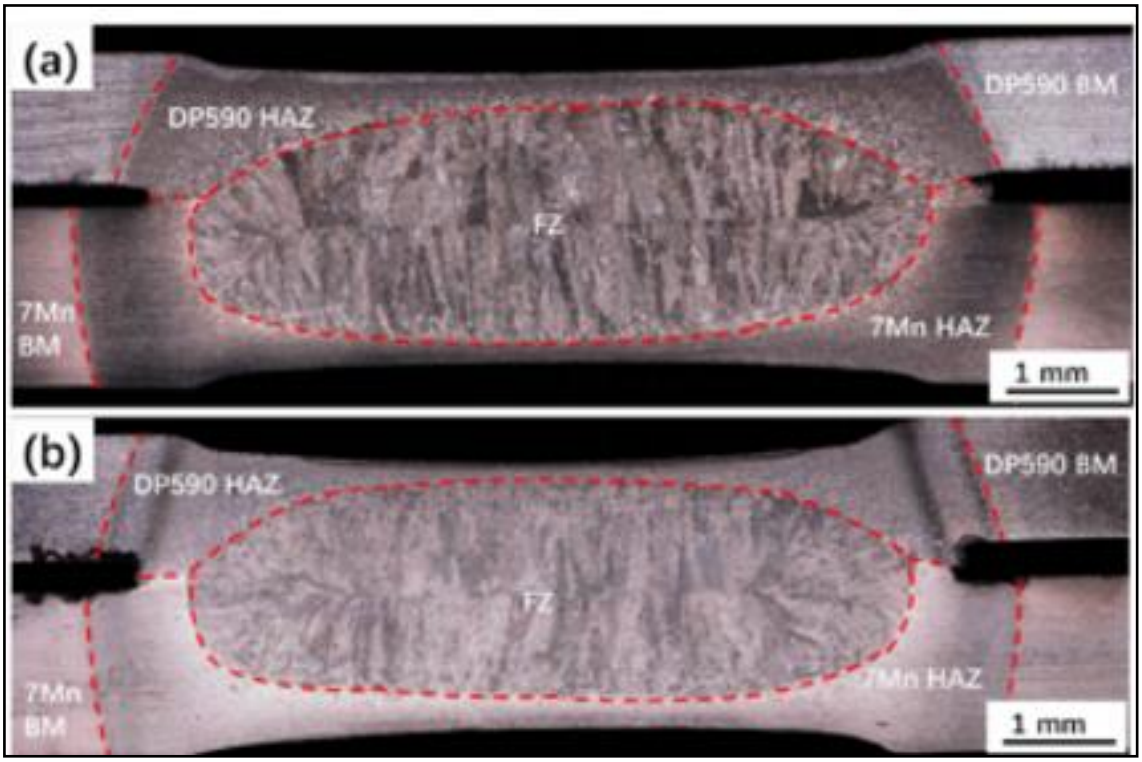

Figure 2-9: Cross section of resistance spot welding joints (a) single pulse (b) double pulse [19]

Internal stresses such as residual stress at the nugget weld can be reduced dramatically with this heat treatment. Because of this, the second pulse can be named as tempering current. After applying the tempering current, microstructure became more uniform. This can change the failure mode of the resistance spot welding joint in the desired direction as seen in the Figure 2-10.

Even if the failure mode does not change, the heat created by the second pulse current provides resistance to higher forces in service thanks to the neck formation due to the decrease in the hardness in the temper zone at heat effected zone. This means that the resistance spot weld joint is strengthened.

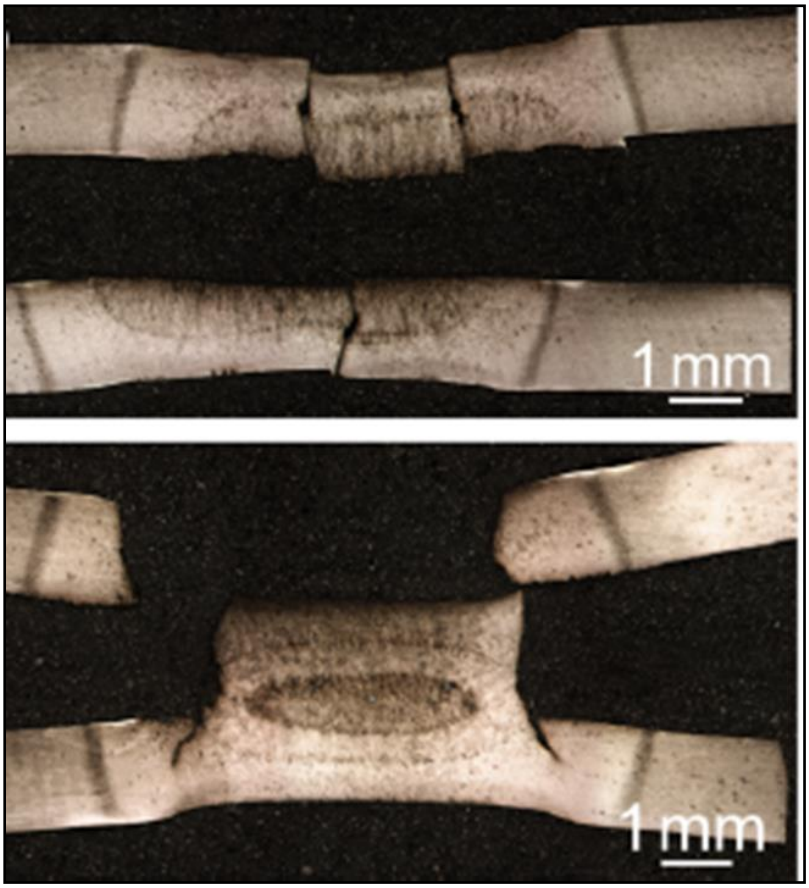

Figure 2-10: Cross section of failed joints: (a) single pulse (b) double pulse [20]

3. MOTIVATION AND METHODOLOGY

3.1. Motivation

Resistance spot welding is a very complex process that is used to permanently assemble two or more metals together with the energy generated by converting electrical current into heat energy. The main purpose of this study is understanding and optimizing resistance spot welding process in advanced high strength steels to obtain the desired welding joint properties, strength and failure mode by using both single pulse resistance spot welding and double pulse spot welding methods. The difference of this study from other studies in literature is that this study examines the properties of the resistance spot welds obtained from joining the advanced high strength steel with dual-phase steel and unalloyed mild steel using a secondary supporting welding current with experimental modelling approach.

3.2. Methodology

3.2.1. Materials

During this experimental modeling study, steels with different physical properties and different chemical compositions are used to examine the effect of double pulse resistance spot welding on steels generally used in the automotive industry. In this way, it is possible to evaluate the effects of double pulse resistance spot welding on different types of steel-steel interface combinations separately. The tensile tests of the materials used in the study are carried out and their physical properties were calculated in terms of the average values and standard deviations of all samples. These physical properties will be shared in "Experimental Results" section. In addition, the chemical composition of the steels used, published by the manufacturer, will be tabulated below.

The first of the steels used is the unalloyed steel named DD11, which is one of the hot rolled mild carbon steels. DD11 has a wide range of uses in the industry. Common uses of DD11 include solid transmission parts, vibration dampers, brake pistons and similar components. The chemical composition of DD11 steel can be seen in Table 3-1.

Table 3-1: Chemical composition of DD11 mild unalloyed steel

	C [%]	**Mn [%]**	**P [%]**	**S [%]**	**Al [%]**
DD11	0.057	0.219	0.011	0.016	0.045

The second steel used in the study is DP800 steel, which is one of the dual-phase steels used extensively in the automotive industry. Dual-phase steels are subjected to heat treatment during their manufacture in order to meet both the requirements of good ductility and durability, which are indispensable for automobiles.

Although DP800 mainly shows ferritic and martensitic properties, it can also contain small amount of bainite. While the martensitic structure enables the material to reach high strengths, the ferritic structure contributes to its machinability. The chemical composition of DP800 steel can be seen in Table 3-2.

Table 3-2: Chemical composition of DP800 dual-phase steel

	C [%]	**Si [%]**	**Mn [%]**	**P [%]**	**S [%]**	**Al [%]**	**Nb+ Ti [%]**	**Cr+ Mo [%]**	**Cu [%]**
DP800	0.128	0.203	1.39	0.012	0.006	0.036	0.055	0.055	0.0031

The third and last steel used in this experimental modelling study is the martensitic MS1500 steel. MS1500 is one of the strongest members of the family of advanced high strength steels. MS1500 is generally used in structures such as impact beam where crashworthiness and survivability are extremely important.

Providing light weight design without sacrificing durability due to its advanced high strength can be achieved with MS1500 and similar advanced high strength steels. The chemical composition of martensitic MS1500 steel can be seen in Table 3-3.

Table 3-3: Chemical composition of MS1500 martensitic steel

	C [%]	**Si [%]**	**Mn [%]**	**Al [%]**	**Ti [%]**	**Cr [%]**	**B [%]**	**Cu [%]**
MS1500	0.271	0.207	0.77	0.268	0.036	0.023	0.010	0.116

3.2.2. Tensile-Shear Strength Test Specimen

Two different combinations of three metals which are DD11, DP800 and MS1500 steels are used in the study of the experimental modeling of resistance spot welding on advanced high strength steels. In this way, it is possible to evaluate the characteristics of the weld nugget resulting from resistance spot welding of an advanced high strength steel with both a mild steel and a dual-phase steel.

During the preparation of the tensile-shear strength test specimen, 1.2 mm thick sheet metals are used for the MS1500 steel. For both DD11 and DP800 steels, 2 mm sheet metal is used. As the first sample set of the study, DD11 and MS1500 metals are resistance spot welded to each other, while DP800 and MS1500 metals were welded in the second sample set.

Tensile-shear test was used for the mechanical testing of spot welds. Although the Tensile-shear test is a very simple and fast method, it can be easily used for the determination of strength, failure energy and failure mode. In addition, the scatter rate in the results is also very low.

Different thicknesses of sheet metals can cause an alignment problem on sheet metals during tensile-shear strength (TSS) testing. Since the alignment problem may cause sheet bending on the sheet metals and adversely affect the test results, it is appropriate to apply shim on sheet metals to eliminate the thickness difference in order to prevent this situation.

Tensile-shear strength test specimens were prepared in accordance with ISO 14273 standards. The schematics of the samples can be seen in Figure 3-1 and Figure 3-2.

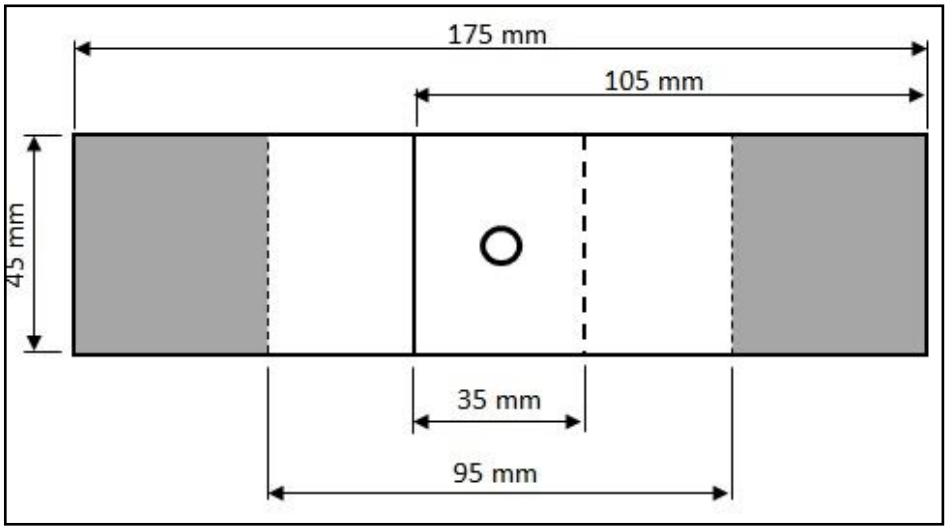

Figure 3-1: ISO 14273 standard specimen top view

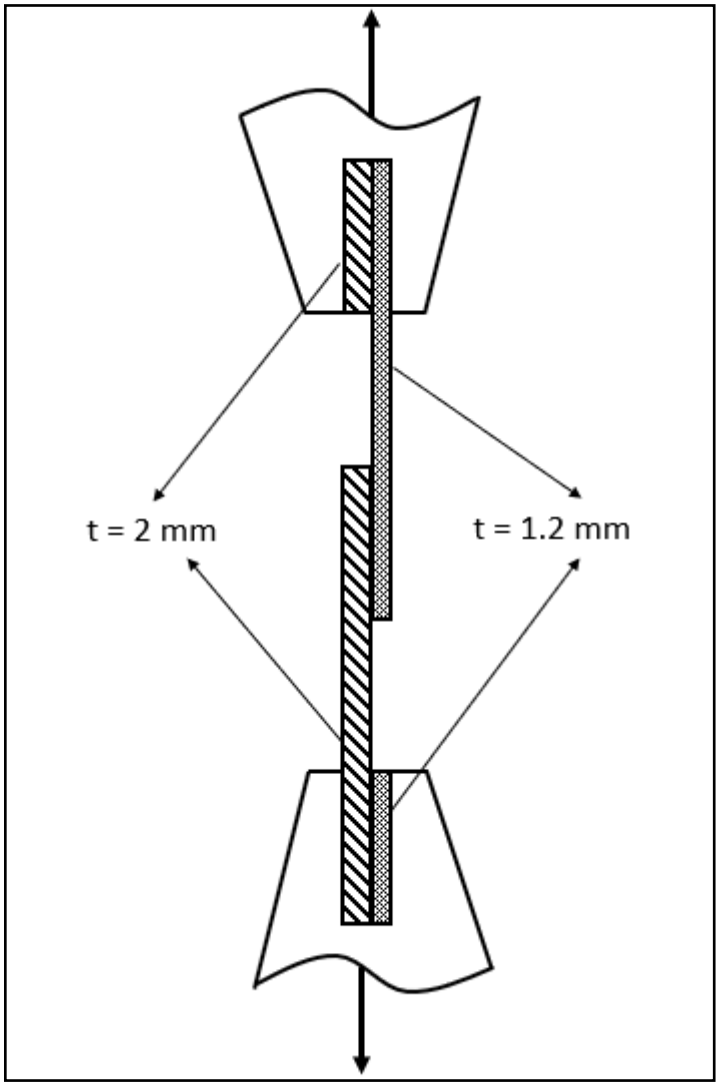

Figure 3-2: ISO 14273 standard specimen profile view with shim plates

3.2.3. Resistance Spot Welding Machine

In this study, the pedestal type AC (50 Hz) resistance spot welding machine shown in the Figure 3-3 is used. Pedestal type spot welding machine stands out not only with its high rigidity and robustness, but also with its high repeatability and minimal loss features. The disadvantage of the pedestal type spot welding machine is that it is inflexible.

Figure 3-3: Pedestal type AC resistance spot welding machine used in study

All samples prepared within the scope of the study were made with a pedestal type resistance spot welding machine in the mechanical fatigue laboratory of Hacettepe University Mechanical Engineering building. The power of the machine is 70 kVA and it is equipped with a CNC controller. Working principle schematic of a standard resistance spot welding machine can be seen in Figure 3-4.

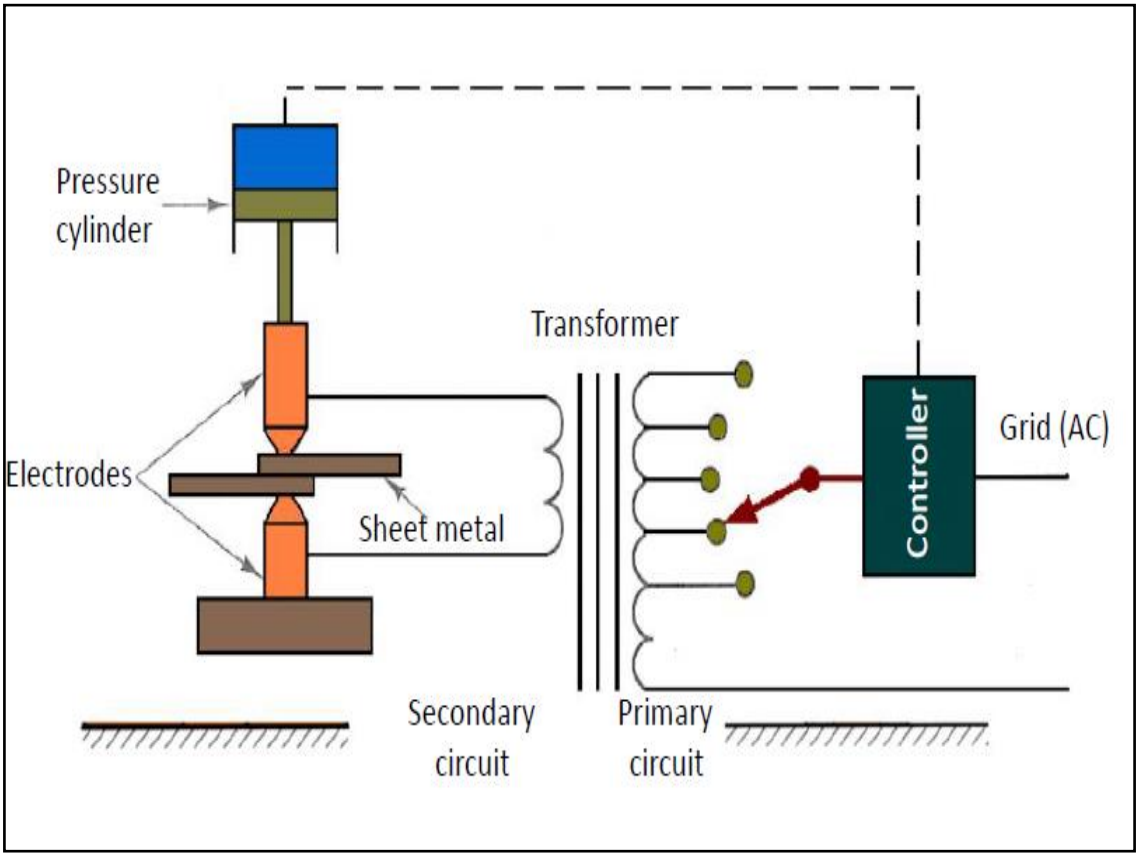

Figure 3-4: Schematic view of resistance spot welding machine

According to Li et al. (2014) [21], pointed type electrode, can be seen in Figure 3-5, with suitable diameter according to the surfaces and metals to be resistance spot welded is sufficient to make the weld size larger than $4\sqrt{t}$ in general applications. In this study, resistance spot welding operations was conducted with using a pointed type resistance welding manufacturers alliance class 2 chromium zirconium copper electrodes. Face diameters of electrodes are 8 mm.

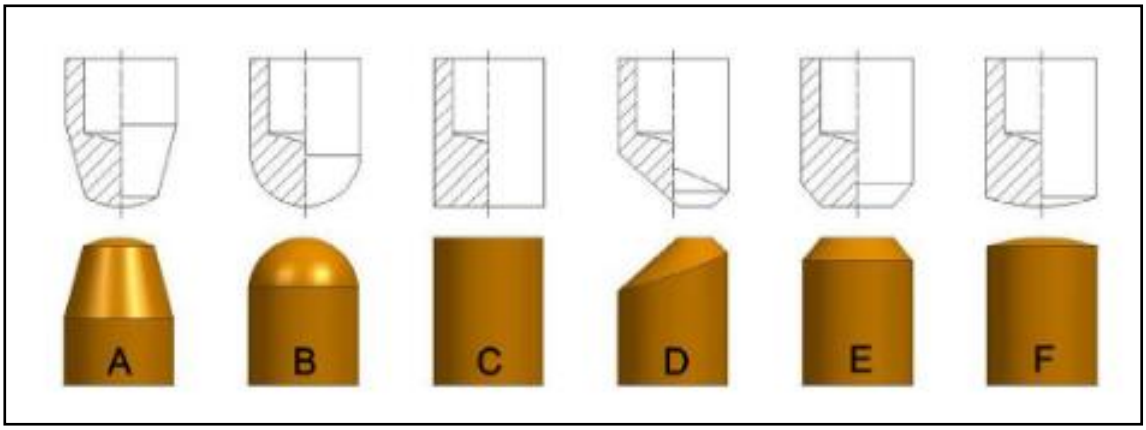

Figure 3-5: Typical shapes of resistance spot welding electrodes (a) pointed (b) dome (c) flat (d) offset (e) truncated (f) radius [21]

3.2.4. Experimental Procedure

During the experimental modeling of resistance spot welding on advanced high strength steels, it is aimed to examine the physical, macro and microstructures of the joint, which is formed as a result of welding one advanced high strength steel with a mild steel and a dual-phase steel to each other.

Electrode force was used as a constant 3.4 kN value during all welding processes. 50 Hz frequency European electric is used during welding operation. 50 Hz and 12 cycles (equivalent to 240 ms) resistance spot welding current applied for each in all pulses, regardless of whether they were first or second pulse.

3.2.4.1. Experimental Procedure of MS1500 – DD11 Specimens

As the first stage of the experimental study, MS1500 and DD11 steels were welded to each other with resistance spot welding based on the ISO 14273 sample. First, a single pulse resistance spot welding process was performed, and it was desired to determine the upper electrical current limit value for expulsion that will occur during welding of MS1500 and DD11 to each other.

Experiments were started to determine expulsion limit of the configuration with a current of 7.2 kA and the current was increased by 0.4 kA in each trial. Since intense expulsions are observed during resistance spot welding processes using 9.2 kA, the maximum welding current for single pulse welding was determined as 8.8 kA, which is just below the critical electrical current, for the consistency of experimental results. Thus, the preparation of single pulse samples to be used in the experimental study was completed.

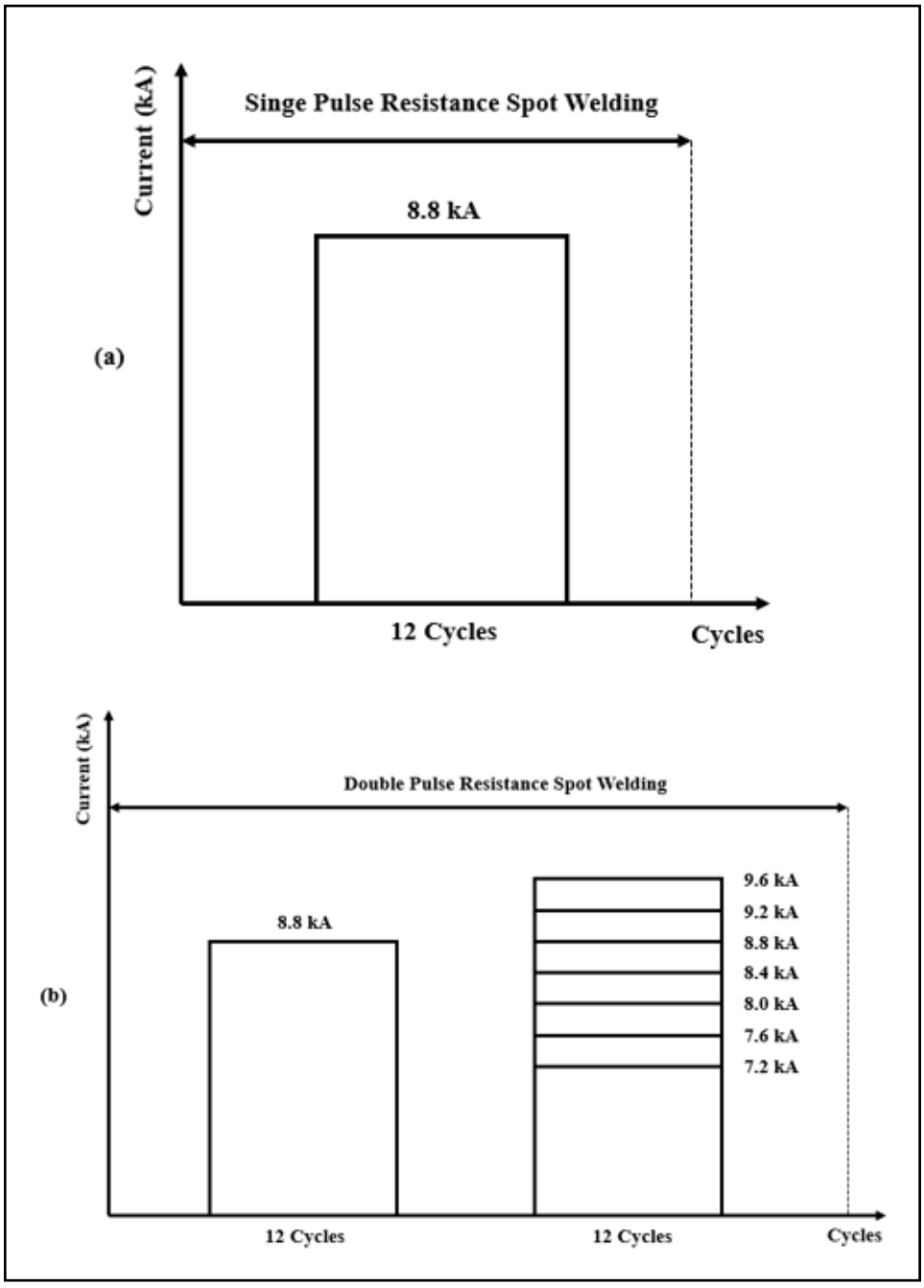

Figure 3-6: Schematic representation of sample preparations of (a) single pulse (b) double pulse resistance spot welding for MS1500 - DD11 steels

8.8 kA electrical current was fixed as the first pulse to be used in the continuation of the experiments. For the second pulse, 7 different sample sets were prepared starting from 7.2 kA current and up to 9.6 kA current with 0.4 kA intervals. A schematic visualization of the current parameters used in the preparation of the samples can be found in the Figure 3-6.

Note that, although an electric current is applied above the critical expulsion limit determined for single pulse resistance spot welding, expulsion is less likely to occur in the second pulse. Kim et al. (2019) [15] states that, the reason for this situation is increase in the contact area after the first pulse. Thanks to the molten material after the first pulse, the roughness on the surface decreases and the effective contact area of the two metals increases. In this way, current flow pattern between the faying surfaces changes. Therefore, both the nugget size increases, and the electrical current value expected to be where expulsion occurs is shifted to a higher value. This phenomenon was observed in both MS1500 – DD11 and MS1500 – DP800 samples. The visual schematization of this phenomenon is shown in the Figure 3-7.

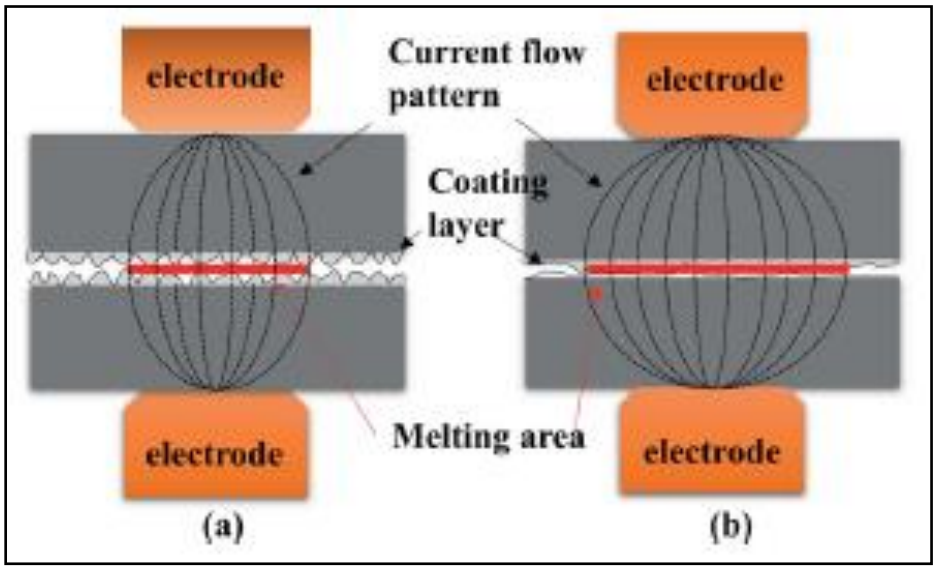

Figure 3-7: Schematic of the current flow pattern difference between (a) high surface roughness and (b) low surface roughness [15]

3.2.4.2. Experimental Procedure of MS1500 – DP800 Specimens

In the second stage of the experimental study, the procedure applied for MS1500 – DD11 samples was also applied for MS1500 – DP800 samples.

Upper electrical current limit value for expulsion that will occur during welding of MS1500 and DP800 to each other for single pulse resistance spot welding was observed as 8.6 kA. So, the maximum welding current for single pulse welding was determined as 8.2 kA, which is just below the critical electrical current, for the consistency of experimental results.

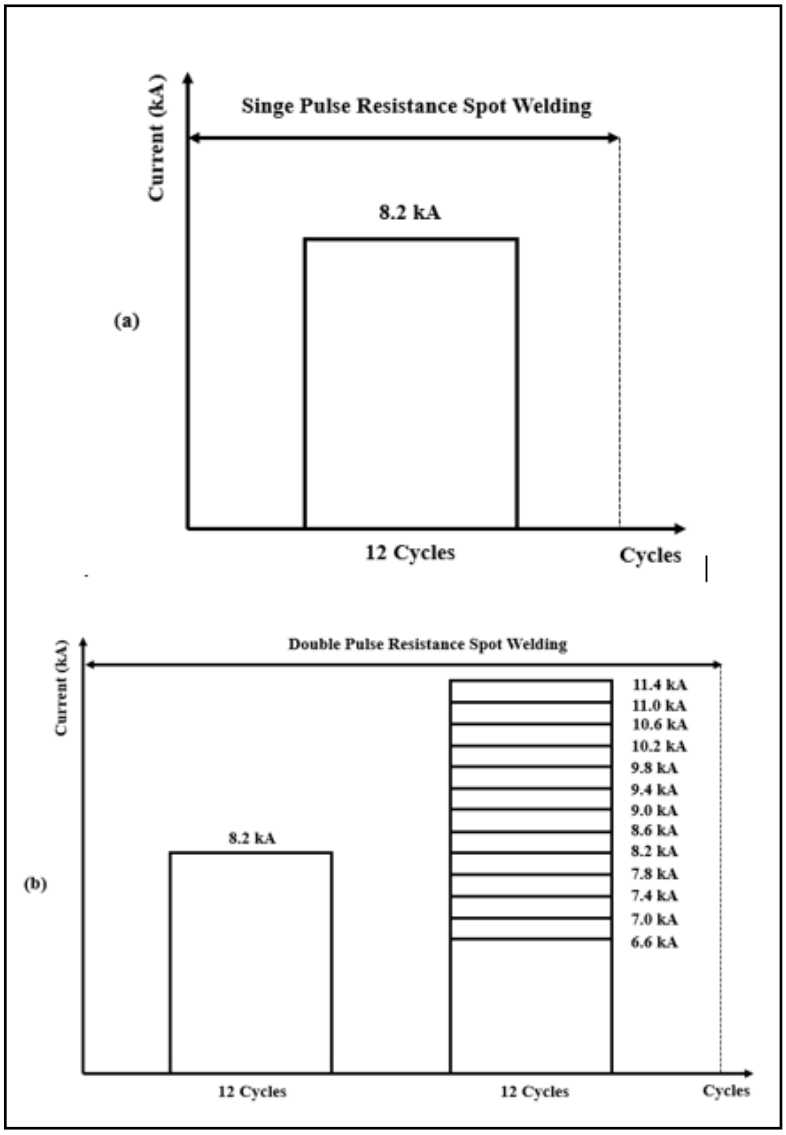

Figure 3-8: Schematic representation of sample preparations of (a) single pulse (b) double pulse resistance spot welding for MS1500 – DP800 steels

8.2 kA electrical current was fixed as the first pulse to be used in the continuation of the experiments. For the second pulse, 13 different sample sets were prepared starting from 6.6 kA current and up to 11.4 kA current with 0.4 kA intervals. A schematic visualization of the current parameters used in the preparation of the samples can be found in the Figure 3-8.

3.2.5. Specimen Preparation

As another step of the experiment process, one sample from each of the 22 sample sets prepared was reserved for examination in a scanning electron microscope and for hardness tests. The remaining samples were used to determine the strength and failure modes of the resistance spot welds formed with using tensile-shear strength.

In order for the sample to be ready for examination, the sample must be cut right in the middle of the nugget surface of the weld. The cross sections of the welded samples were cut from the middle of the nugget surfaces using the MetSPre KC Series Abrasive Cutting Machine.

Figure 3-9: MetSPre KC Series Abrasive Cutting Machine

After the cross sections are taken, the areas that will not be used in further analysis were also cut in order to reduce the samples sizes. Then, each sample was first marked and then mounted in bakelite in pairs. All samples were cold casted using epoxy resin and epoxy curing agent. The primary purpose of the bakelite mounting process is to make amorphous and hard-to-hold parts suitable for examination under the microscope. Another purpose is to protect it from deformations that may occur on important corners, edges and surfaces during sample preparation.

Then, the surfaces of the samples were made bright and smooth by using Metkon FORCIPOL 2V modular grinding and polishing machine. During the grinding process, Silicon Carbide Sandpapers (SIC) with grits P400, P600, P1000 and P2500 were used, respectively. Afterwards, the samples were polished with using 6 μ and 1 μ monocrystalline diamond suspensions respectively. Polished samples can be seen in Figure 3-10.

Figure 3-10: Samples after polishing

After the polishing process, the etching process was applied to the cross sections of the samples. A solution consisting of 4% nitric acid by volume was used for etching. The visuals of the samples with the etching process can be seen in the Figure 3-11: Samples after etching. After etching process, the weld nugget has become easily observable.

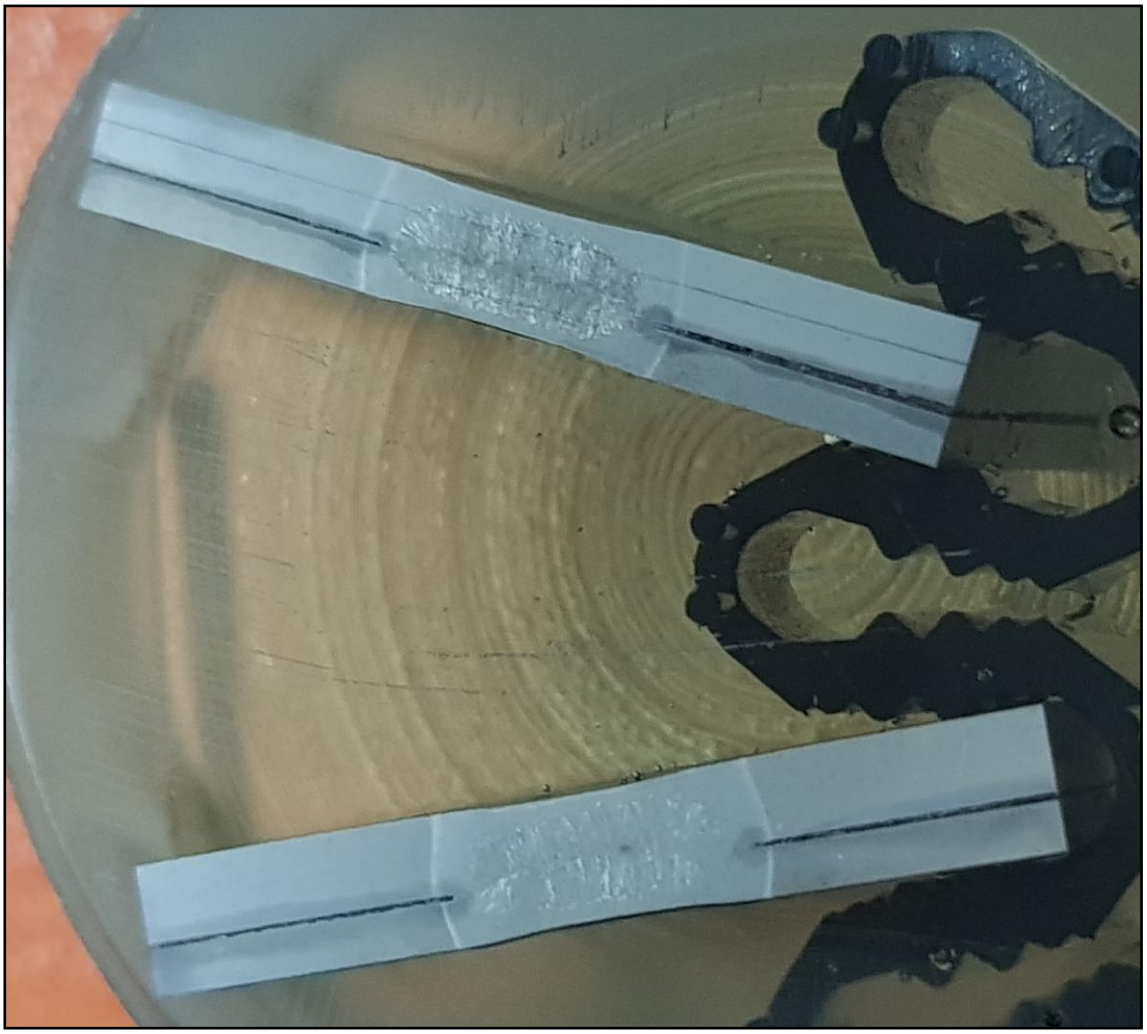

Figure 3-11: Samples after etching

4. EXPERIMENTAL RESULTS

4.1. Mechanical Properties of Materials Used

Tensile test specimens of DD11, DP800 and MS1500 sheet metals used during the experimental modeling study were prepared. Yield strength, ultimate tensile strength, and elongation values obtained from the tensile test results are given in the tables below.

Some of the mechanical properties of DD11 obtained as a result of the tensile tests carried out within the scope of the study are also shown in Table 4-1.

Table 4-1: Mechanical properties of DD11 mild unalloyed steel

DD11	**Yield Strength [MPa]**	**Ultimate Tensile Strength [MPa]**	**Elongation [%]**
Average	272.27 ± 3.89	372.26 ± 3.11	34.48 ± 0.79

Some of the mechanical properties of DP800 obtained as a result of the tensile tests carried out within the scope of the study are also shown in Table 4-2.

Table 4-2: Mechanical properties of DP800 dual-phase steel

DP800	**Yield Strength [MPa]**	**Ultimate Tensile Strength [MPa]**	**Elongation [%]**
Average	718.40 ± 12.63	922.23 ± 6.54	16.63 ± 0.43

Some of the mechanical properties of MS1500 obtained as a result of the tensile tests carried out within the scope of the study are also shown in Table 4-3.

Table 4-3: Mechanical properties of MS1500 martensitic steel

MS1500	Yield Strength [MPa]	Ultimate Tensile Strength [MPa]	Elongation [%]
Average	1459.00 ± 37.97	1643.85 ± 24.67	5.47 ± 0.81

4.2. Resistance spot welding of MS1500 and DD11

4.2.1. Tensile-Shear Strength Results of MS1500 and DD11

DD11 and MS1500 sheet metals were resistance spot welded to each other in accordance with the test procedure described in "Section 3.2.4.1.". Tensile-shear strength tests were applied to the obtained samples in a tensile test setup. In addition to the durability of the resistance spot welds formed after welding, the failure modes were also examined.

The tensile test results of the samples consisting of DD11 and MS1500 sheet metals are shown in Figure 4-1. Tensile-Shear Strength values were taken as the highest load values seen during the tests. Failure energy values, on the other hand, were obtained by calculating the area under the diagram between the no-load state to the highest load.

The bar diagrams on the Figure 4-1 show the tensile-shear strength and failure energy values. The lines represent the standard deviation amounts in the tensile-shear strength and failure energy values of the test samples.

When the failure mode analysis of the samples, which experienced fracture after the tensile test, were performed, it was observed that the failure mode types of the samples in the experiment set were different from each other. The tendency to failure was detected as interfacial failure in the samples with single pulse resistance spot welding. Interfacial failure is the most undesirable type of failure in resistance spot welding applications. In a welded joint with interfacial failure, the strength of the welded joint is lower than the materials on which the welding process is made, and such a failure mode is desired to be avoided, especially in the automotive industry.

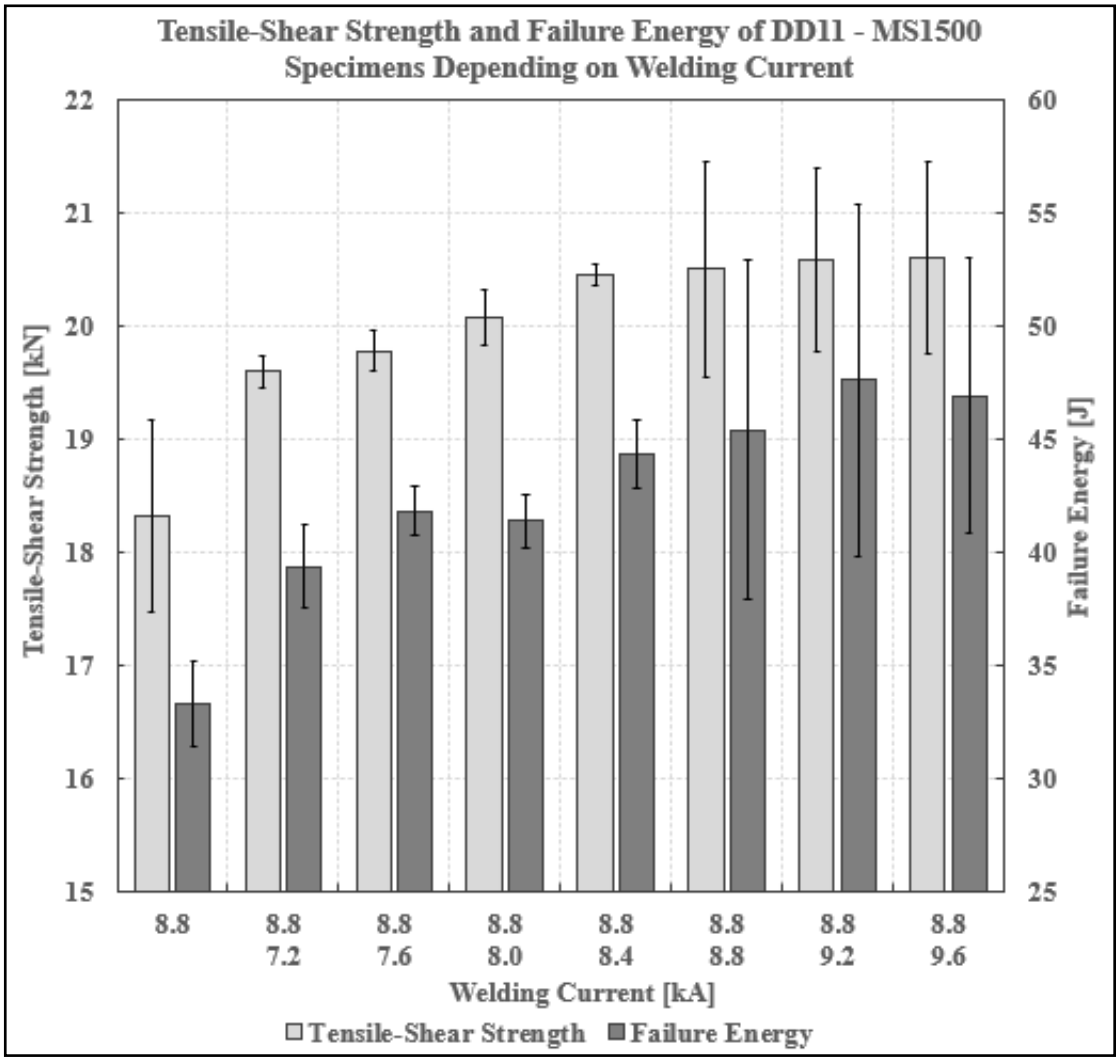

Figure 4-1: Tensile-Shear Strength and Failure Energy of DD11-MS1500 Specimens Depending on Welding Current

To get rid of the interfacial failure mode, the nugget diameter needs to be enlarged. For this, it is necessary to increase the welding current. However, the main reason for choosing 8.8 kA welding current as a single pulse welding current was that this value was just below the expulsion limit in the welding of MS1500 and DD11 metals. In other words, without expulsion of MS1500 and DD11 metals under these experimental parameters (electrode force, electrode geometry, welding time etc.), it does not seem possible to switch from interfacial failure mode to another failure mode without a complementary second pulse application. Therefore, the application of second pulse resistance spot welding seems necessary to increase the strength of the welding.

When looking at the test samples in which double pulse resistance spot welding was performed, it was observed that there was a transition from the interfacial failure mode to the pullout failure and pullout failure followed by base metal tearing modes, respectively, depending on the amount of increase in the second pulse value. But after the secondary current value exceeds a certain amount, expulsion is observed. As a result, a decrease in the strength of the joint is normally expected.

Figure 4-2: Failure modes of resistance spot welding samples (a) interfacial failure (single pulse 8.8 kA) (b) pullout failure (8.8 – 7.2 kA) (c) pullout failure followed by base metal tearing (8.8 – 8.4 kA) (d) pullout with expulsion (8.8 – 9.2 kA)

When the second pulse welding current is 7.2 kA, pullout failure occurs. When the second pulse value is increased to 8.4 kA, pullout failure followed by base metal tearing mode can now be seen easily. If 9.2 kA value is reached by continuing to increase the current, the expulsion effect is now clearly observed. The cross-section visuals of four selected samples representing the welding current increases from interfacial failure mode to expulsion can be seen in the Figure 4-2. In addition, the characteristic load displacement diagram for the selected samples can be seen in the Figure 4-3.

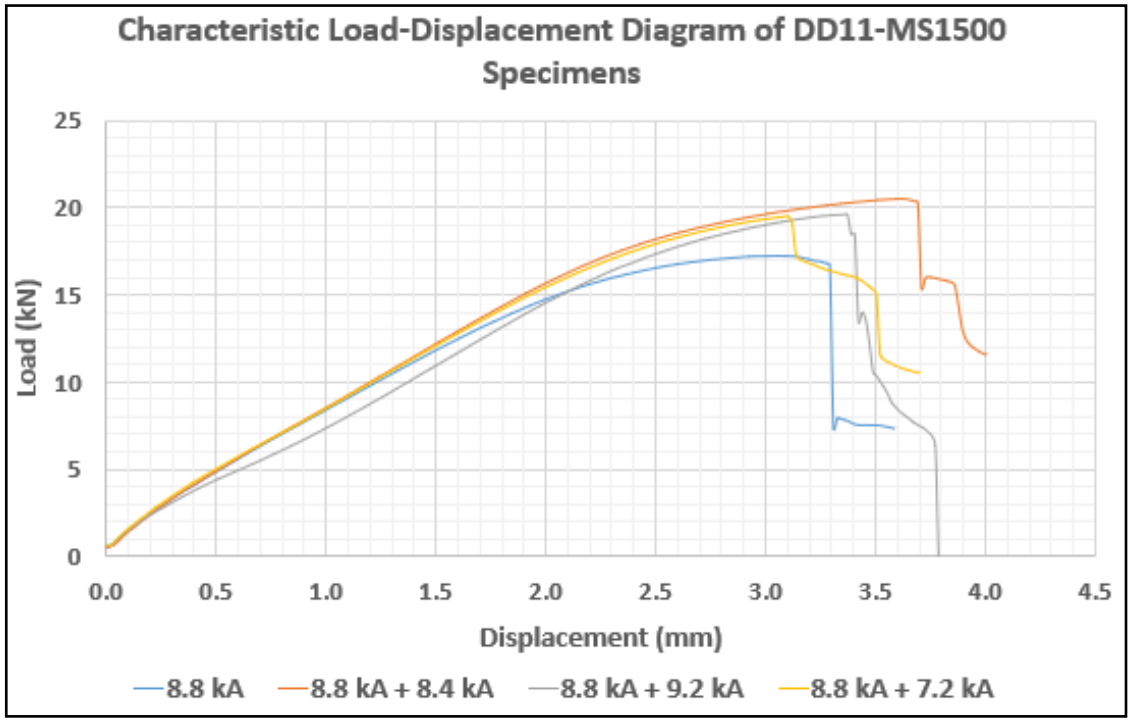

Figure 4-3: Characteristic Load-Displacement Diagram of DD11-MS1500 Specimens

4.2.2. Tensile-Shear Strength Results of MS1500 and DP800

DP800 and MS1500 sheet metals were resistance spot welded to each other in accordance with the test procedure described in “Section 3.2.4.2.”. Tensile-shear strength tests were applied to the obtained samples in a tensile test setup. In addition to the durability of the resistance spot welds formed after welding, the failure modes were also examined.

The tensile test results of the samples consisting of DP800 and MS1500 sheet metals are shown in Figure 4-4. The bar diagrams on the Figure 4-4 show the tensile-shear strength and failure energy values. The lines represent the standard deviation amounts in the

tensile-shear strength and failure energy values of the test samples. Tensile-shear strength and failure energy values were calculated with the same method as DD11 and MS1500 samples.

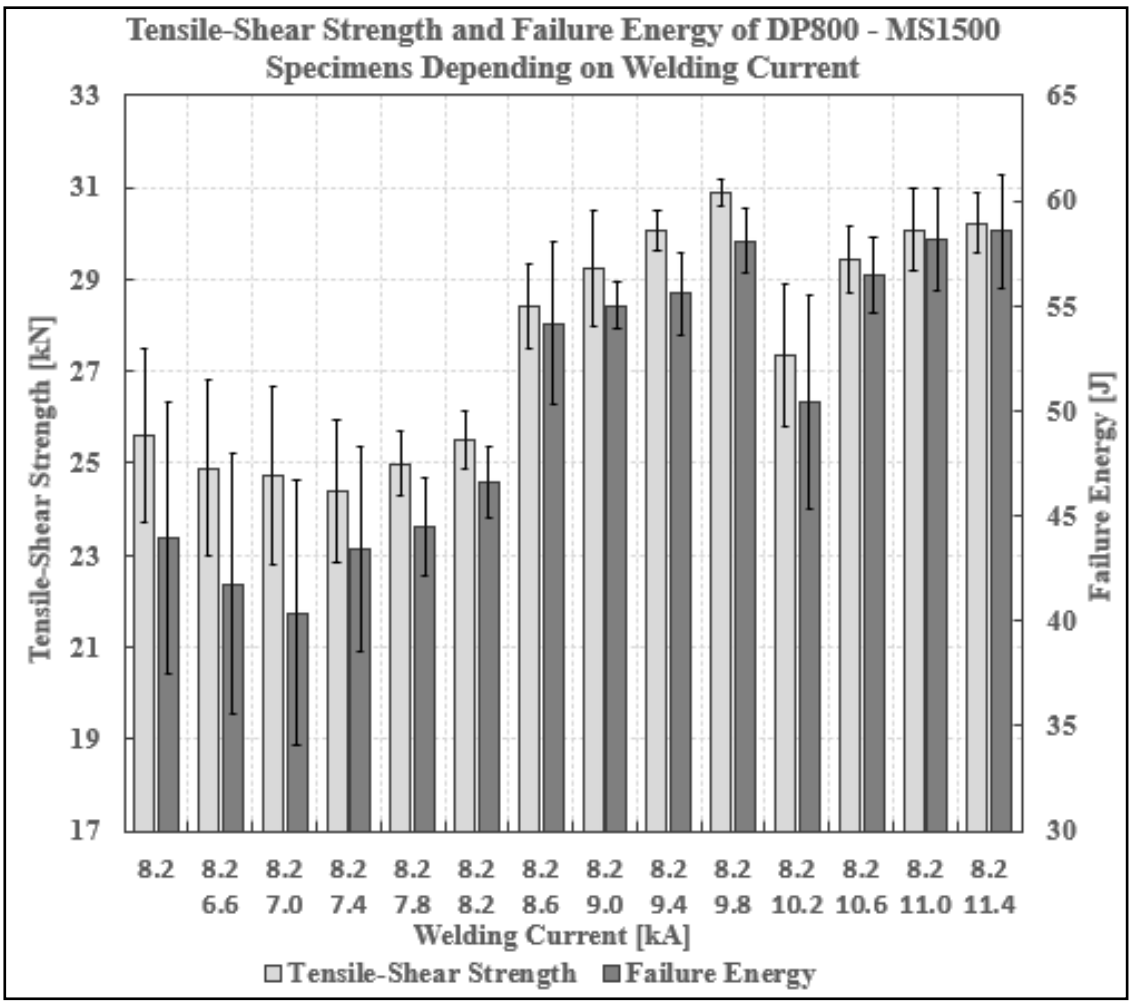

Figure 4-4: Tensile-Shear Strength and Failure Energy of DP800-MS1500 Specimens Depending on Welding Current

The tendency to failure was detected as interfacial failure in the samples with single pulse resistance spot welding. When looking at the test samples in which double pulse resistance spot welding was performed, it was observed that there was a transition from the interfacial failure mode to the partial pullout failure and pullout failure modes, respectively, depending on the amount of increase in the second pulse value. But after the secondary current value exceeds a certain amount, expulsion is observed.

When the second pulse welding current is 8.2 kA, partial pullout failure occurs. When the second pulse value is increased to 9.8 kA, pullout failure mode can now be seen. If 10.2 kA value is reached by continuing to increase the current, the expulsion effect is now clearly observed. The cross-section visuals of four selected samples representing the welding current increases from interfacial failure mode to expulsion can be seen in the Figure 4-5. In addition, the characteristic load displacement diagram for the selected samples can be seen in the Figure 4-6.

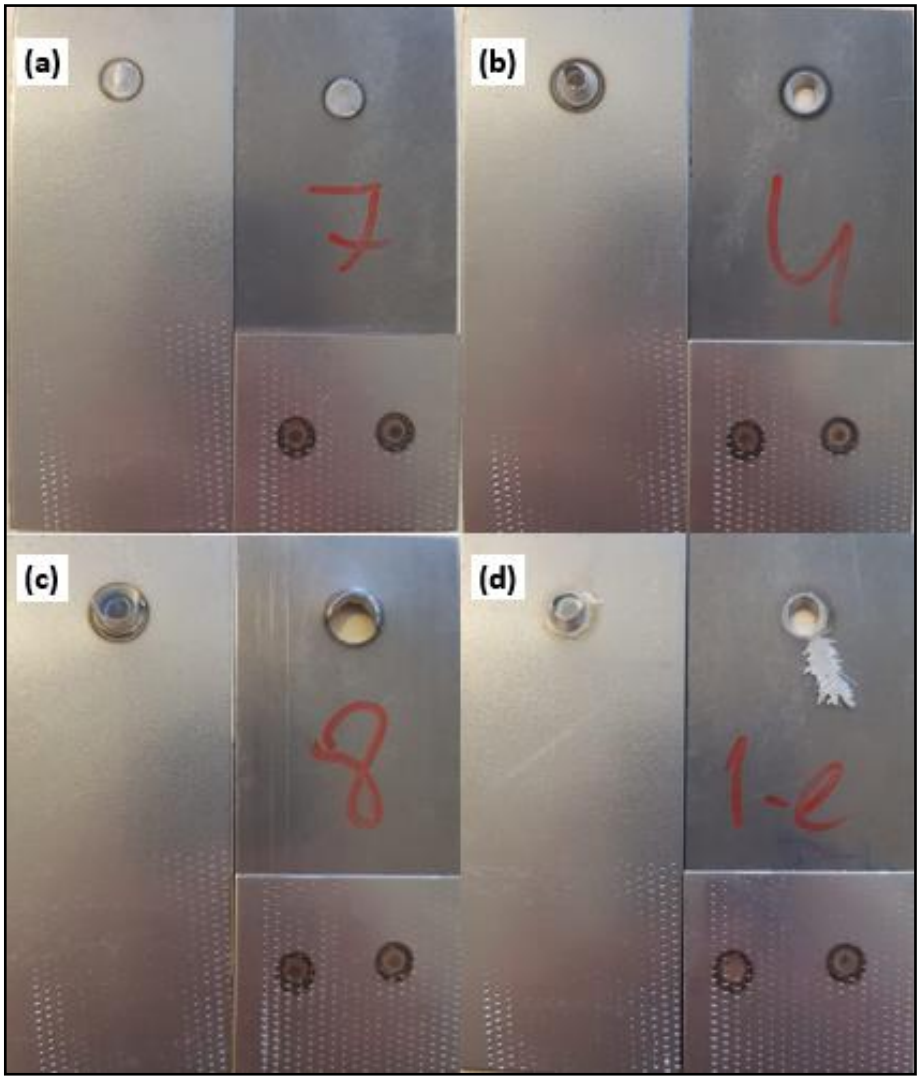

Figure 4-5: Failure modes of resistance spot welding samples (a) interfacial failure (single pulse 8.2 kA) (b) partial pullout failure (8.2 – 8.2 kA) (c) pullout failure (8.2 – 9.8 kA) (d) pullout with expulsion (8.2 – 10.2 kA)

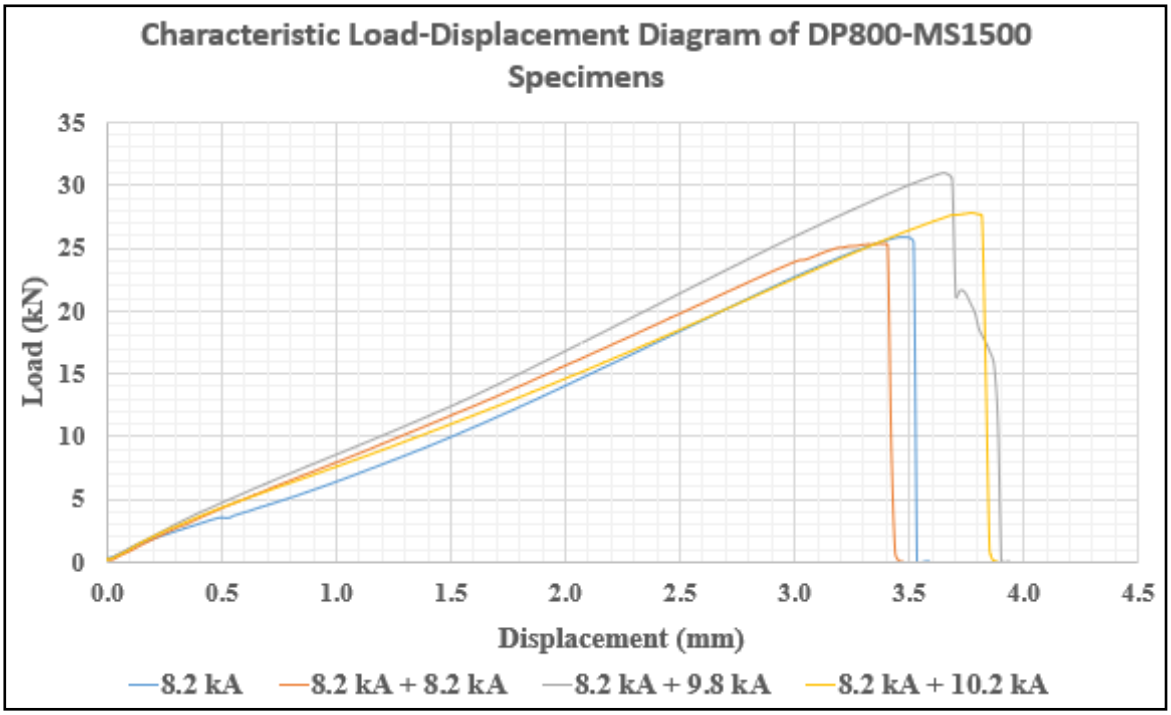

Figure 4-6: Characteristic Load-Displacement Diagram of DP800-MS1500 Specimens

4.3. Geometric Dimensions of Weld Nugget

Measurements of some geometric dimensions, which determine the strength and quality of the weld zone, were made on the samples whose nuggets became easily observable after etching. These geometric dimensions were measured as nugget size (width), nugget height on each material and total indented thickness after resistance spot welding process, respectively. A sample resistance spot welding nugget dimensions measurement from each of the two sample sets can be found in Figure 4-7 and Figure 4-8.

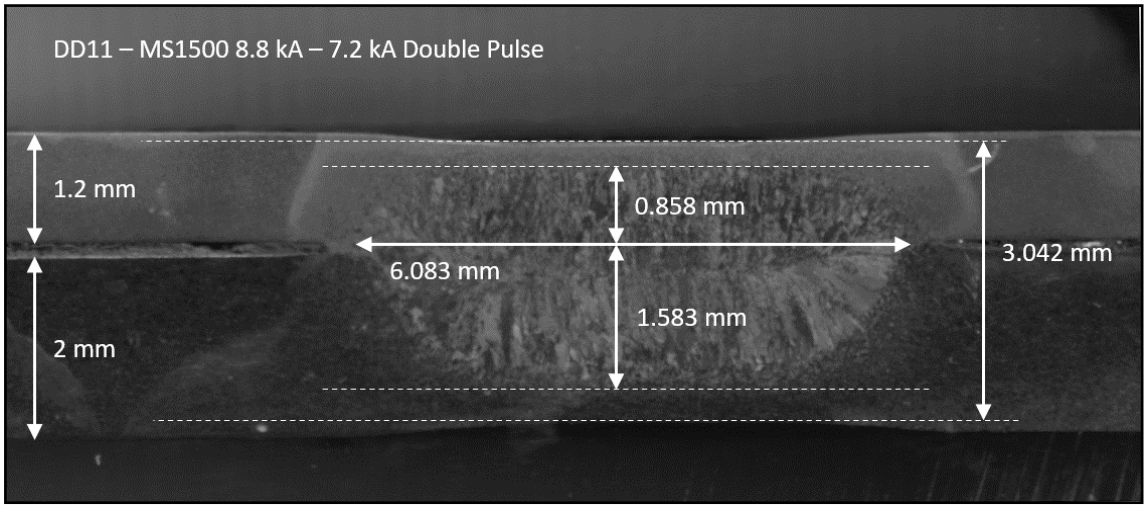

Figure 4-7: Weld nugget dimensions of DD11-MS1500 8.8 kA – 7.2 kA double pulse sample

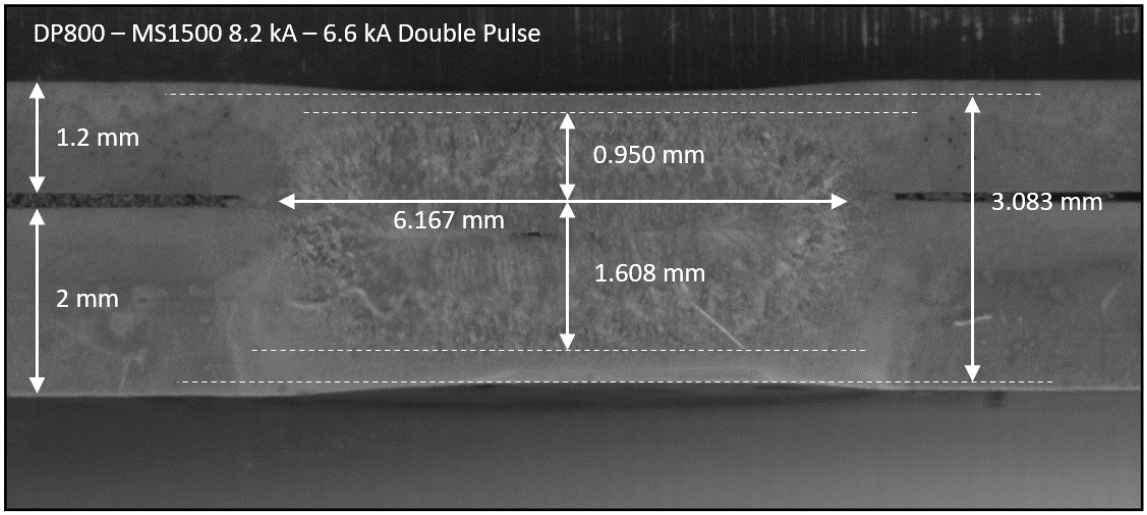

Figure 4-8: Weld nugget dimensions of DP800-MS1500 8.2 kA – 6.6 kA double pulse sample

4.3.1. DD11 and MS1500

Nugget sizes of DD11-MS1500 specimens can be seen in Figure 4-9. Nugget height on DD11 and MS1500 materials given in Figure 4-10 and Figure 4-11, separately. Finally, total indented thickness is shown in the Figure 4-12.

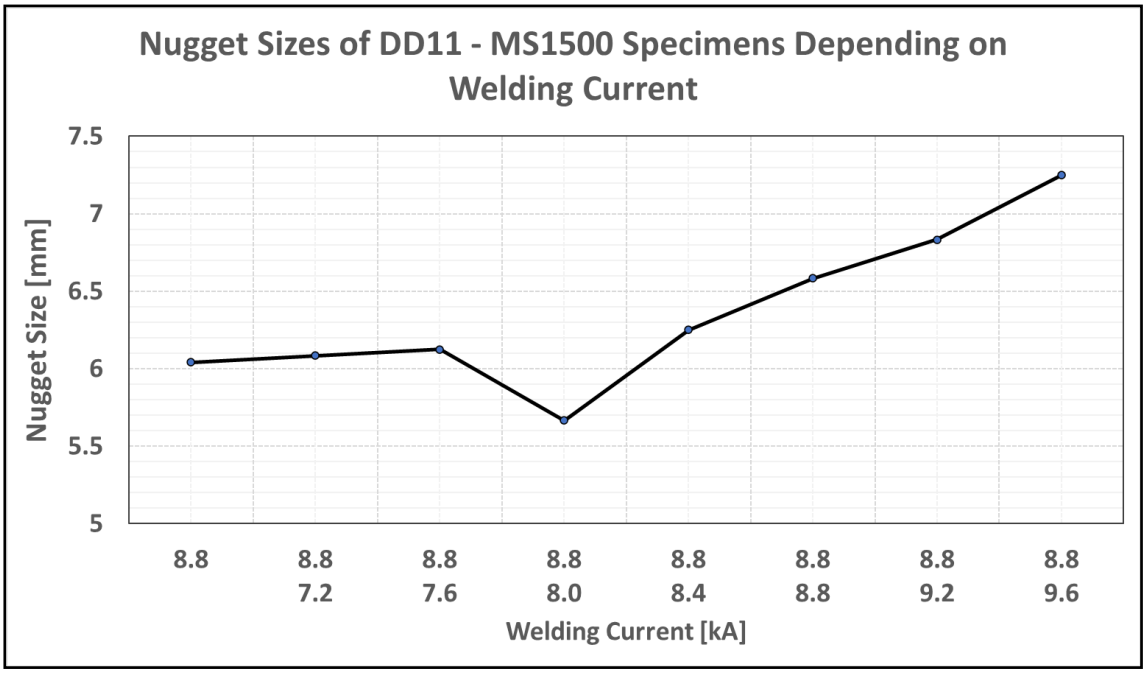

Figure 4-9: Nugget sizes of DD11-MS1500 specimens depending on welding current

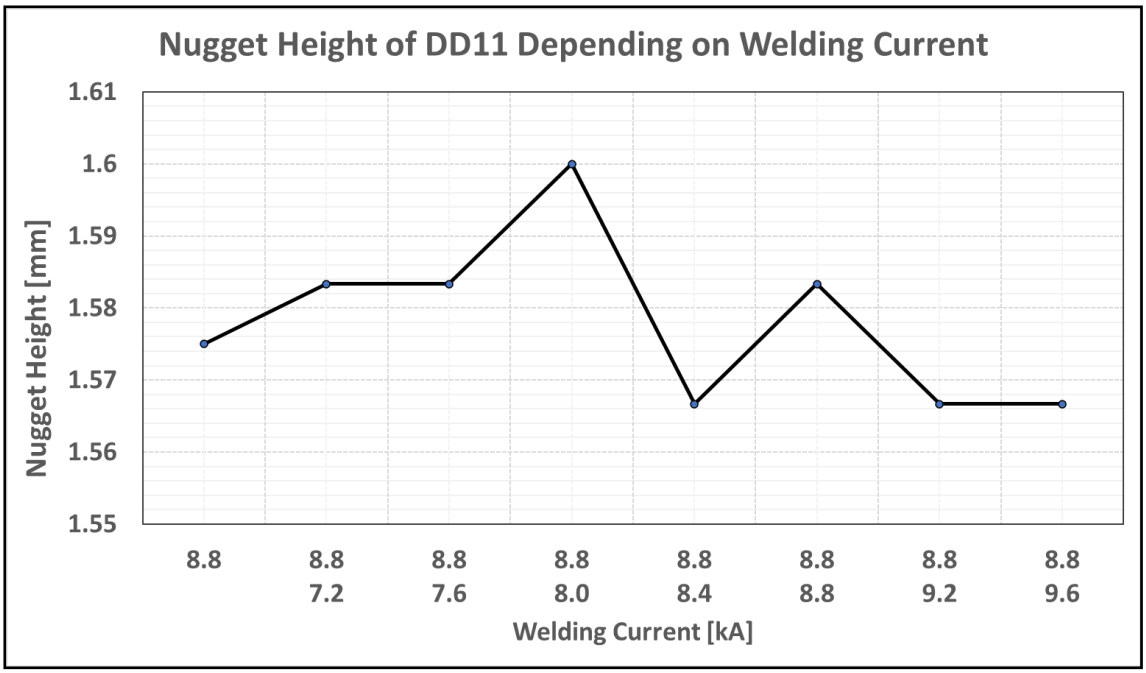

Figure 4-10: Nugget height on DD11 material side

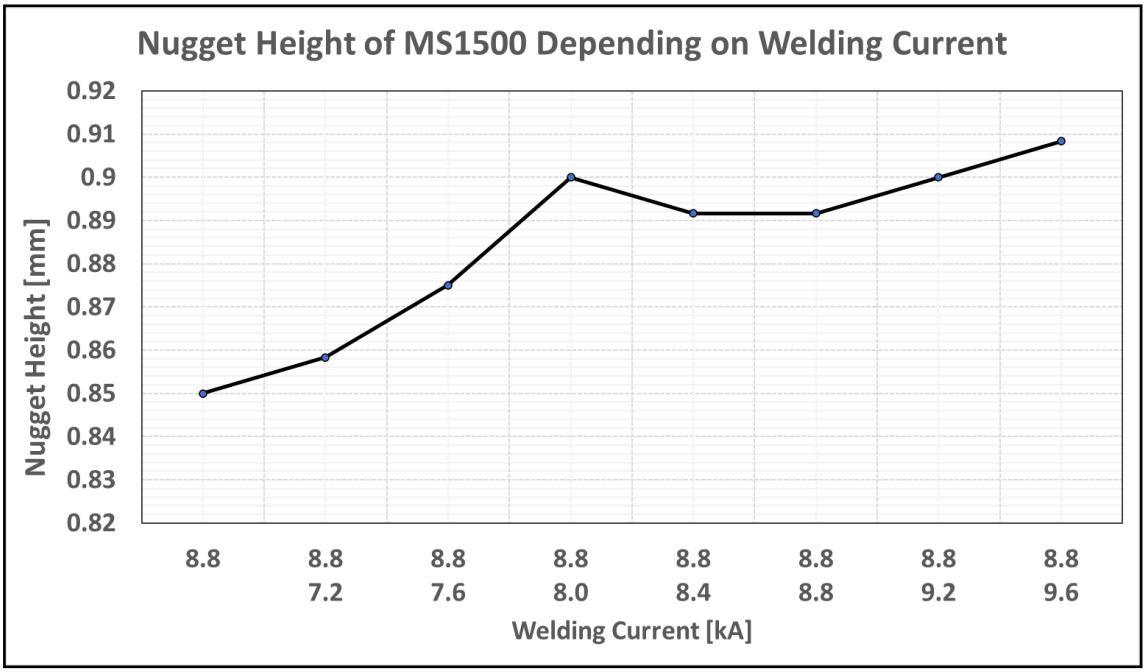

Figure 4-11: Nugget height on MS1500 material side

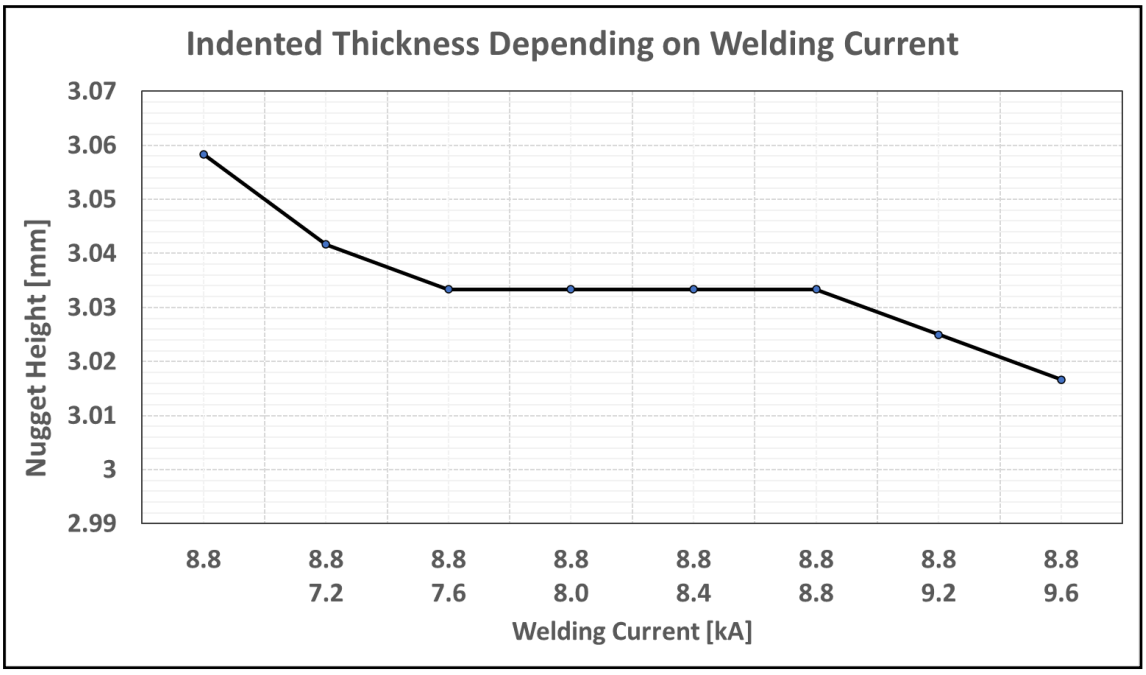

Figure 4-12: Total indented thickness on nugget weld region of DD11-MS1500 specimens

It should be noted that as the secondary current value increases, the total energy increases in direct proportion to the square of the current value. In this way, the nugget width tends to increase gradually. The total indented thickness, on the other hand, first decreases to a certain extent under the effect of the applied force as a result of the softening of the material in the fusion zone during resistance spot welding. After it is fixed up to a certain current value, it continues to decrease following the decrease of the total material because of expulsion in the nugget area.

4.3.2. DP800 and MS1500

Nugget sizes of DP800-MS1500 specimens can be seen in Figure 4-13. Nugget height on DP800 and MS1500 materials given in Figure 4-10 and Figure 4-11, separately. Finally, total indented thickness is shown in the Figure 4-12.

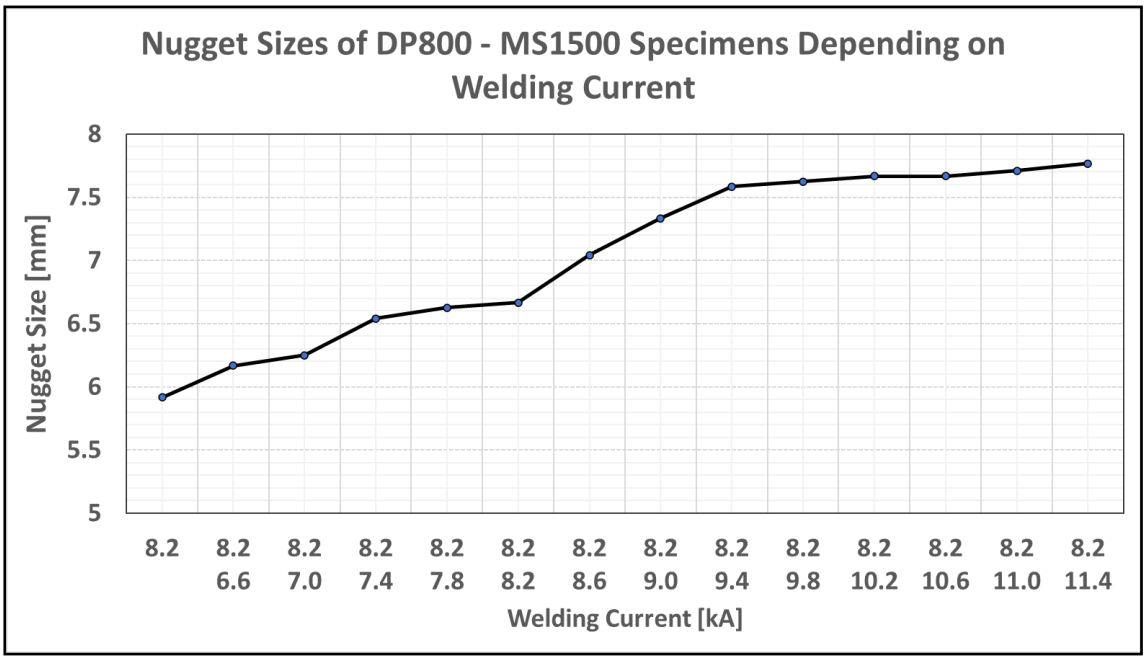

Figure 4-13: Nugget sizes of DP800-MS1500 specimens depending on welding current

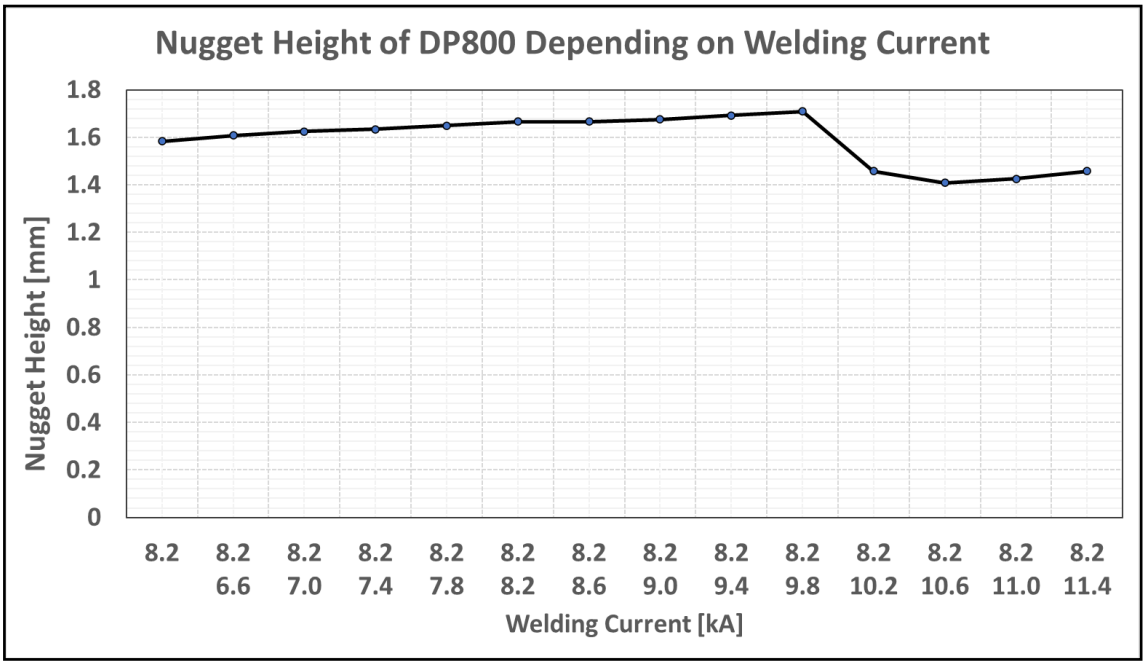

Figure 4-14: Nugget height on DP800 material side

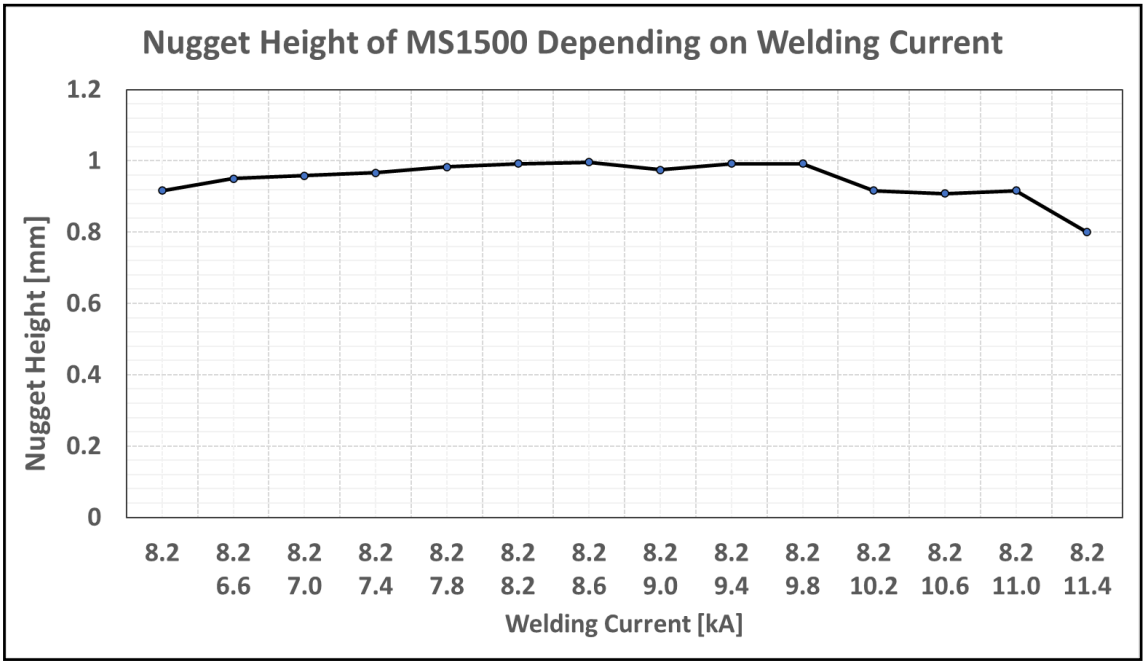

Figure 4-15: Nugget height on MS1500 material side

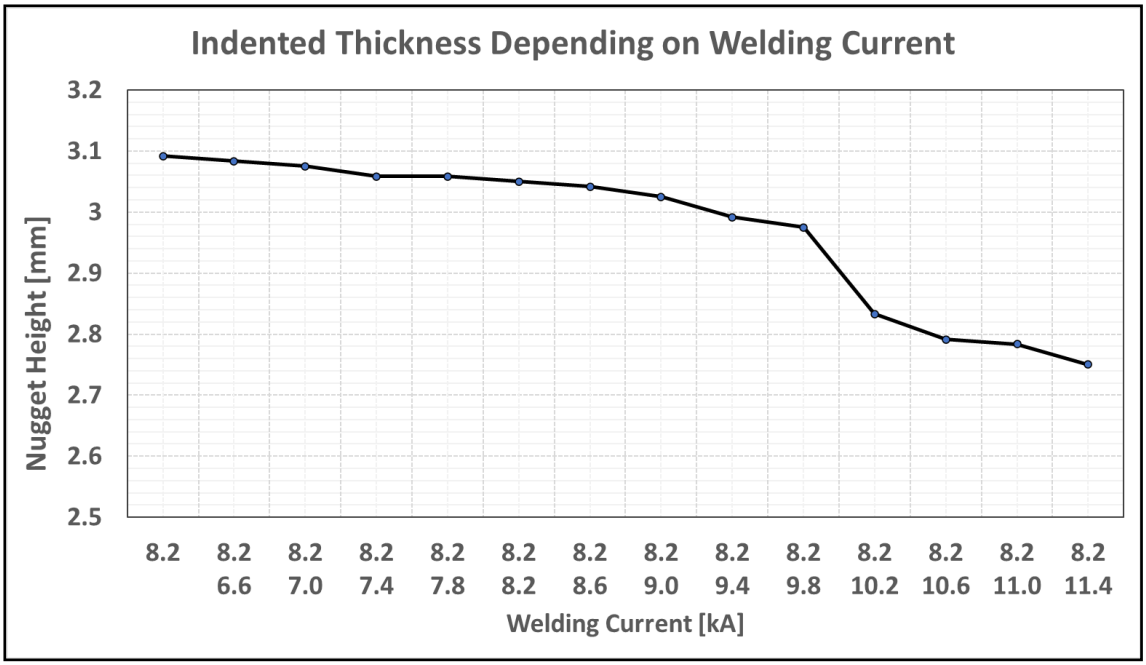

Figure 4-16: Total indented thickness on nugget weld region of DP800-MS1500 specimens

Similar comments made for the DD11-MS1500 samples, can also be made for DP800-MS1500 samples. When the second pulse current value increases, the nugget width tends to increase gradually, as expected. The total indented thickness, on the other hand, decreases to a certain extent under the effect of the applied force as a result of the softening of the material in the fusion zone during resistance spot welding. After a certain second pulse current, at that current value expulsion is experienced, the rate of decrease in the total indented thickness value increases.

4.4. Hardness Results

Microhardness measurements are made along the weld area from some selected samples. During these measurements, two sets of measurements are taken 0.35 mm above and below the separation point of the two materials. In this way, the microhardness values of both materials can be determined throughout the weld area.

Measurements are taken at 0.25 mm intervals, starting 0.5 mm before and after the start and end of the heat affected zone. Vickers microhardness tests with a load of 500 g and dwell time of 15 s are used for microhardness measurements.

While measuring the hardness, the sample produced with 8.8 kA-8.4 kA double pulse from DD11-MS1500 samples is used. Of the DP800-MS1500 samples, 8.2 kA single pulse, 8.2 kA-7.0 kA and 8.2 kA-9.8 kA double pulse samples are used. In this way, both the different behavior of different kind of steel types during resistance spot welding operation can be examined and the change in hardness can be observed due to the increase in secondary current with double pulse application.

In Figure 4-17, the hardness distribution values of the DD11-MS1500 sample across the nugget are given. In Figure 4-18 and Figure 4-19, the hardness values of the DP800-MS1500 samples can be seen throughout the nugget.

From the DD11-MS1500 metal pair, a significant increase in hardness value is observed during the transition from the base metal region to the heat affected zone (HAZ) region of the martensitic steel MS1500 metal, whose strength is considerably higher than the DD11. Afterwards, the metal became annealed and lost some of its harness. In the nugget region, the MS1500 melted together with DD11, which has a very low hardness value, and formed a homogeneous martensitic structure whose hardness drops to approximately 400 HV. Almost the same hardness value can be observed in the nugget region of DD11 metal. Looking at the hardness profile of the DD11 metal outside the nugget zone, a sharp increase in the HAZ is also observed.

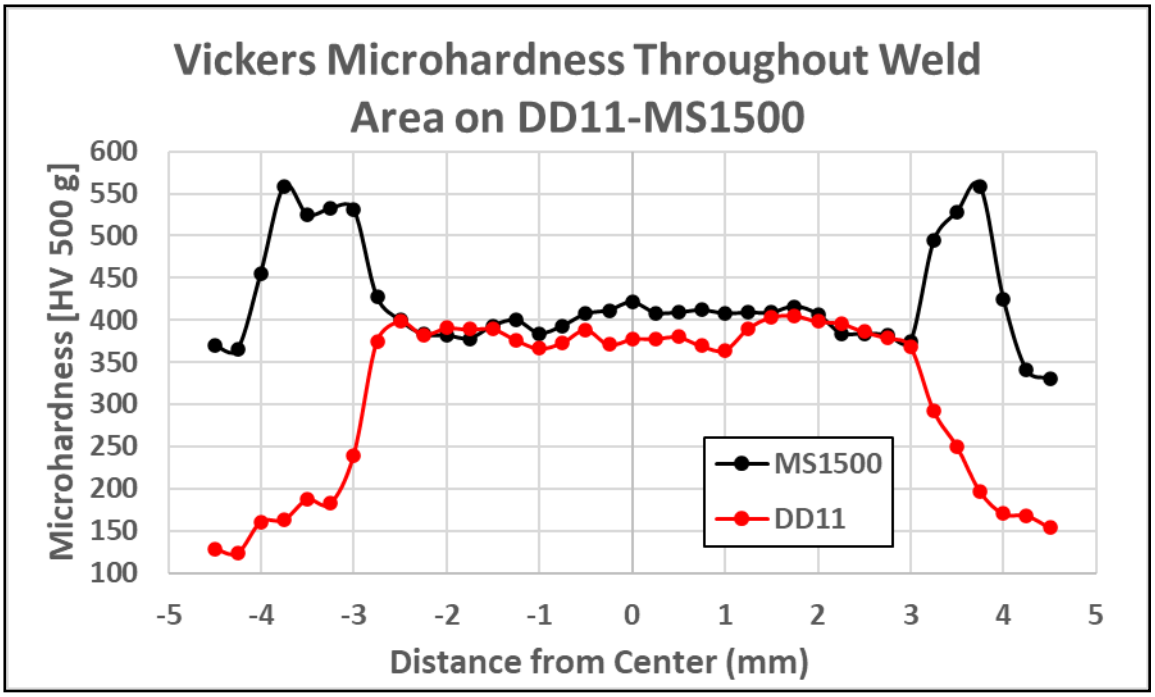

Figure 4-17: Vickers microhardness values of MS1500 and DD11 throughout weld area on DD11-MS1500 8.8 kA – 8.4 kA double pulse specimen

Similar comments are valid for the hardness distributions in the nugget regions of the samples obtained from the DP800-MS1500 metal pairs. Since the base metal hardness of DP800 steel is higher than that of DD11, the average hardness value in the homogeneous martensitic nugget region is approximately 450 HV, which is higher than that of the DD11-MS1500 sample. With the double pulse current application, there was no noticeable change in the hardness value of the metals in the nugget region compared to the single pulse current application. Likewise, increasing the secondary pulse current value does not change the hardness value. These applications only have an effect on the increase in total nugget size value.

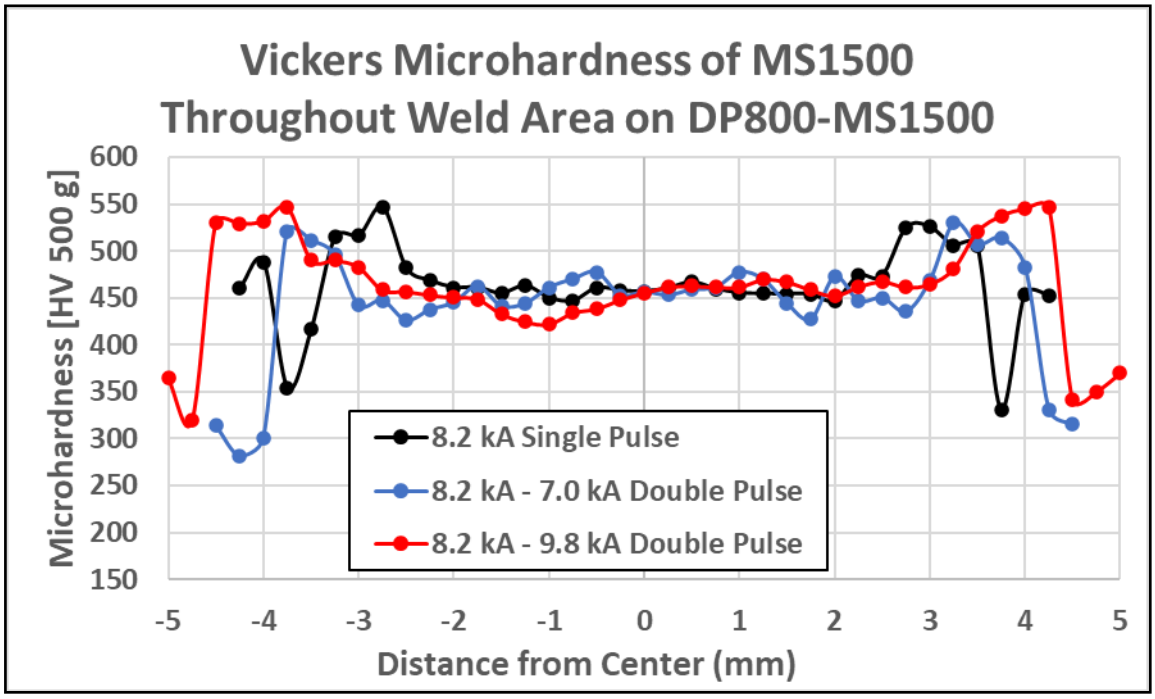

Figure 4-18: Vickers microhardness of MS1500 throughout weld area on DP800-MS1500 specimens

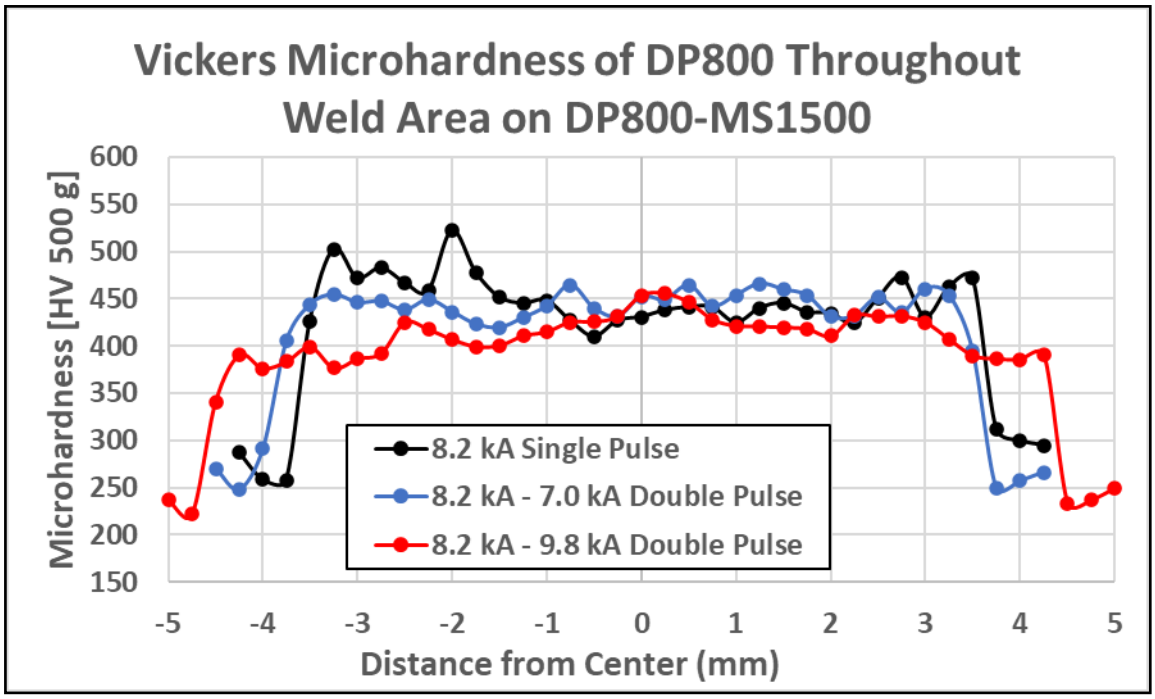

Figure 4-19: Vickers microhardness of DP800 throughout weld area on DP800-MS1500 specimens

5. CONCLUSIONS AND OUTLOOK

In this study, resistance spot welding of advanced high strength steels has been experimentally modeled and investigated in detail. The materials used during the experimental studies are MS1500 martensitic steel with 1.2 mm sheet thickness and DP800 and DD11 metals with 2 mm sheet thicknesses each. In this study, the strength values and failure mode behaviors of the welding joint resulting from joining MS1500 AHSS metal with an unalloyed mild steel and a dual-phase steel using resistance spot welding were investigated. For both specimen sets, two resistance spot welding with single and double pulse current applications were examined.

In both types of sample sets, applied current values are just below the expulsion limit during the single pulse application. It can be said that a significant increase was observed in tensile-shear strength and failure energy values with double pulse resistance spot welding application. Looking at the DD11-MS1500 samples, in the second welding current values, starting from 7.2 kA to 8.4 kA, both the tensile-shear strength and failure energy of the welding joint increase and the deviations in test results between samples decreases. The tensile-shear strength value, which was 18.32 kN in single pulse 8.8 kA welding current application, increased by 11.6 % and increased to 20.45 kN in double pulse 8.8 kA-8.8 kA samples. Likewise, the failure energy value increased by 33.2 % from 33.27 J to 44.32 J. In terms of failure modes, the interfacial failure seen in the single pulse application has changed to the pullout failure mode, which is the desired failure mode in the double pulse 8.8 kA-8.4 kA application.

Looking at the DP800-MS1500 samples, the tensile-shear strength value, which was 25.61 kN on average in the single pulse 8.2 kA application, increased by 20.1 % to 30.89 kN in the double pulse 8.2 kA-9.8 kA samples. Likewise, the failure energy value increased by 32.1 % from 43.97 J to 58.09 J. Starting from single pulse 8.2 kA, failure mode changed from interfacial mode to pullout mode until 9.8 kA, which is the highest second pulse current value with no expulsion formation observed.

It can be said for both DD11-MS1500 and DP800-MS 1500 specimen sets that although the nugget size increased as a result of increasing the second current value further, it did not provide a noticeable increase in the tensile-shear strength value, but it increased the deviation in the tensile-shear strength values between the samples tested with the same parameters due to the resulting expulsion.

When the hardness test results were evaluated, no remarkable difference was observed in the hardness value in the nugget region between the single pulse application and the double pulse application. Also, it was determined that the increase in the second current value did not cause any change in the hardness value in the nugget region.

As a result of the study, it can be said that the welding current in the single pulse application can only be increased a certain amount until expulsion is experienced in the joining process of martensitic steels with mild unalloyed steel and dual-phase steels with resistance spot welding. Naturally, the increase in nugget size and the associated strength of the welding joint are limited. It has been observed that the application of double pulse resistance spot welding can provide a significant increase in the strength of the joint. For assembly process of DD11-MS1500 metal pairs, 8.8 kA-8.4 kA double pulse resistance spot welding application was determined as the most appropriate application in terms of strength and consistency of the welding joint. Similarly, 8.2 kA-9.8 kA double pulse resistance spot welding provides optimum strength and consistency results for the DP800-MS1500 metal pair assembly.

6. REFERENCES

1. World Auto Steel. (2021, November 29). Advanced High-Strength Steel (AHSS) Definitions. WorldAutoSteel. https://www.worldautosteel.org/steel-basics/automotive-advanced-high-strength-steel-ahss-definitions/
2. Jing, Y., Xu, Y., Wang, D., Lu, L., Li, J., & Yu, Y. (2022, May). Improving mechanical properties of welds through tailoring microstructure characteristics and fracture mechanism in multi-pulse resistance spot welding of Q&P980 steel. Materials Science and Engineering: A, 843, 143130. https://doi.org/10.1016/j.msea.2022.143130
3. Cheah LW. Cars on a diet: the materials and energy impacts of passenger vehicle weight reductions in the U.S. Massachusetts Institute of Technology, USA, 2010.
4. Tolouei, R., & Titheridge, H. (2009, August). Vehicle mass as a determinant of fuel consumption and secondary safety performance. Transportation Research Part D: Transport and Environment, 14(6), 385–399. https://doi.org/10.1016/j.trd.2009.01.005
5. Broughton, J. (1996, January). The British index for comparing the accident record of car models. Accident Analysis &Amp; Prevention, 28(1), 101–109. https://doi.org/10.1016/0001-4575(95)00049-6
6. Soomro, I. A., Pedapati, S. R., & Awang, M. (2021, February 8). Double Pulse Resistance Spot Welding of Dual Phase Steel: Parametric Study on Microstructure, Failure Mode and Low Dynamic Tensile Shear Properties. Materials, 14(4), 802. https://doi.org/10.3390/ma14040802
7. Eisazadeh, H., Hamedi, M., & Halvaee, A. (2010). New parametric study of nugget size in resistance spot welding process using finite element method. Materials & Design, 31(1), 149–157.
8. Raoelison, R. N., Fuentes, A., Pouvreau, C., Rogeon, P., Carré, P., & Dechalotte, F. (2014). Modeling and numerical simulation of the resistance spot welding of zinc coated steel sheets using rounded tip electrode: Analysis of required conditions. Applied Mathematical Modelling, 38(9–10), 2505–2521.
9. Pfeifer, M. (2009). Materials Enabled Designs: The Materials Engineering Perspective to Product Design and Manufacturing (1st ed.). Butterworth-Heinemann. https://doi.org/10.1016/B978-0-7506-8287-9.00005-7

10. Groover, M. P. (2010). Fundamentals of Modern Manufacturing: Materials, Processes, and Systems (4th ed.). Wiley.
11. Gupta, O. P., & De, A. (1998). An Improved Numerical Modeling for Resistance Spot Welding Process and Its Experimental Verification. Journal of Manufacturing Science and Engineering, 120(2), 246–251.
12. Zhang, H., & Senkara, J. (2005). Resistance Welding. Taylor & Francis.
13. https://www.jfe-tec.co.jp/en/tech-consul/yosetsu-01c.html
14. Zhao, Y., Zhang, Y., & Lai, X. (2018, September 26). Analysis of Fracture Modes of Resistance Spot Welded Hot-Stamped Boron Steel. Metals, 8(10), 764. https://doi.org/10.3390/met8100764
15. Liu, X., Xu, Y., Misra, R., Peng, F., Wang, Y., & Du, Y. (2019, January). Mechanical properties in double pulse resistance spot welding of Q&P 980 steel. Journal of Materials Processing Technology, 263, 186–197. https://doi.org/10.1016/j.jmatprotec.2018.08.018
16. Kim, J. W., Murugan, S. P., Yoo, J. H., Ashiri, R., & Park, Y. D. (2019, October 21). Enhancing nugget size and weldable current range of ultra-high-strength steel using multi-pulse resistance spot welding. Science and Technology of Welding and Joining, 25(3), 235–242. https://doi.org/10.1080/13621718.2019.1680483
17. Eftekharimilani, P., van der Aa, E., Hermans, M., & Richardson, I. (2017, January 12). Microstructural characterisation of double pulse resistance spot welded advanced high strength steel. Science and Technology of Welding and Joining, 22(7), 545–554.
18. Lee, H. T., & Chang, Y. C. (2020, September 24). Effect of Double Pulse Resistance Spot Welding Process on 15B22 Hot Stamped Boron Steel. Metals, 10(10), 1279. https://doi.org/10.3390/met10101279
19. Wei, F., Zhu, Y., Tian, Y., Liu, H., Zhou, Y., & Zhu, Z. (2022, September 25). Resistance Spot-Welding of Dissimilar Metals, Medium Manganese TRIP Steel and DP590. Metals, 12(10), 1596. https://doi.org/10.3390/met121015964
20. Chabok, A., Cao, H., van der Aa, E., & Pei, Y. (2022, March). New insights into the fracture behavior of advanced high strength steel resistance spot welds. *Journal of Materials Processing Technology*, *301*, 117433. https://doi.org/10.1016/j.jmatprotec.2021.117433

21. Li, Y., Wei, Z., Li, Y., Shen, Q., & Lin, Z. (2013). Effects of cone angle of truncated electrode on heat and mass transfer in resistance spot welding. International Journal of Heat and Mass Transfer, 65, 400–408. https://doi.org/10.1016/j.ijheatmasstransfer.2013.06.012